ABSTRACT OF THE THESIS OF

Jennifer E. DeHart for the degree of Master of Science in Pharmacy presented on July 12, 1996. Title: Partial Purification and Characterization of L-Pipecolic Acid Dehydrogenase from Rabbit Kidney Cortex.

Abstract approved: Redacted for Privacy

T. Mark Zabriskie

L-pipecolic acid (L-PA), a six carbon imino acid, is an intermediate of lysine metabolism in various organisms including bacteria, yeast, fungi, and mammals. In mammals, L-PA catabolism is unusual in that two flavin dependent enzymes have evolved for this process. In primates, the enzyme involved in L-PA degradation, L-pipecolate oxidase (L-PO), has been purified and characterized as a membrane-associated, peroxisomal oxidase possessing a covalent flavin and producing H_2O_2. In lower mammals, L-PA degradation is catalyzed by a soluble, mitochondrial dehydrogenase, but little is known about this enzyme from any source. This thesis describes the partial purification and characterization of L-pipecolic acid dehydrogenase (L-PADH) from rabbit kidney cortex and compares physical and catalytic properties of the rabbit dehydrogenase with those of the primate oxidase.

L-PADH has been purified 300 fold from rabbit kidney cortex. The standard purification procedure included homogenization followed by DEAE-cellulose chromatography and 45% ammonium sulfate precipitation. Chromatography on a Sephadex G-150 size exclusion column preceded hydrophobic interaction chromatography with butyl Sepharose. After dialysis, DEAE Fast Flow chromatography resulted in a final specific activity of 400 $nmol \cdot mg^{-1} \cdot hr^{-1}$.

The pH optimum of L-PADH is 8.5 and the enzyme is an acidic protein with an estimated pI of 5.6. The rabbit dehydrogenase is highly specific for L-PA with a K_m of 0.88 mM and a V_{max} of 20 nmol•mg^{-1}•min^{-1}. Using substrate stereospecifically deuterated at C-6, it was determined that L-PADH abstracts the *pro*-6*R* hydrogen of L-PA.

Sixteen analogs of L-PA were tested as substrates and inhibitors of L-PADH. Unsaturated and sulfur containing analogs provided the best alternate substrates of L-PADH. Nitrogen substituted, oxygen and nitrogen containing analogs served as poor substrates or were not oxidized by L-PADH. Of these sixteen L-PA analogs, no inhibitors were found for L-PADH.

Partial Purification and Characterization of L-Pipecolic Acid Dehydrogenase from Rabbit Kidney Cortex

by

Jennifer E. DeHart

A THESIS

submitted to

Oregon State University

in partial fulfillment of
the requirements for the
degree of

Master of Science

Presented July 12, 1996
Commencement June 1997

Master of Science thesis of Jennifer E. DeHart presented on July 12, 1996

APPROVED:

Redacted for Privacy

Major Professor, representing Pharmacy

Redacted for Privacy

Dean of College of Pharmacy

Redacted for Privacy

Dean of Graduate School

I understand that my thesis will become part of the permanent collection of Oregon State University libraries. My signature below authorizes release of my thesis to any reader upon my request.

Redacted for Privacy

Jennifer E. DeHart, Author

ACKNOWLEDGMENTS

Because research is a cooperative effort and the field of biochemistry requires many technical skills and knowledge, I would like to take this opportunity to express my sincere gratitude to those that helped me through my stay here at Oregon State University.

First and foremost I would like to thank my advisor, Prof. T. Mark Zabriskie. Mark allowed me to venture in my own direction, even when it was an obvious "dead end." Even though we did not see eye to eye on everything, he still believed in me when I didn't even believe in myself. His patience, intellect and support were imperative to my success.

I would also like to thank Dr. Roy LaFever and Prof. Phil Proteau. Dr. LaFever was an important resource in the purification process and helped, with utter enthusiasm, in the isolation procedure using the Preparative Native Gel Electrophoresis equipment and the Rotofor Cell. His friendship and insight are greatly appreciated. Professor Proteau allowed me to use his perfusion column system and answered many questions without complaint or doubt.

My committee members have offered their insight and guidance as well; I would like to thank Prof. Phil McFadden, Prof. Terri Lomax, and Prof. Bill Gerwick. I would also like to thank Prof. Paul Franklin and Prof. Mark Leid of the Pharmacy Department for their assistance with computer problems and the immunoprecipitation, respectively.

Without the support of my fellow labmates I would not have been able to do the inhibitor/alternate substrate studies; my sincere thanks to Mr. Xi Liang and Mrs. Hua Chi for the synthesis of these compounds. I would also like to thank the various other people in the department who have supported me: Barb Hettinger-Smith, Melodie Graber, Mary Roberts, Jim Rossi, Jef Shields, Beth Olenchek, and also my friends outside of the department: DeVon Yoder, Meredith McDonald, Jane Stevens, Jim Pugh, Jeff Schott, Ed

and Gwen Peachy, Beth and Bob Bontrager, Mark Leichty and Ann Detweiler. All of these people offered encouragement and understanding throughout my graduate career.

Lastly, I would like to thank my family for their continuing support even when they didn't understand what I was doing or why. Thanks to my brother, Thomas, who pushed me to my limits and showed me how much I could accomplish. I would like to dedicate this thesis to my parents, Tom and Jo, who supported and encouraged me through the difficult times, and rejoiced with me during the successful times. Their continuing love has been essential for my success.

TABLE OF CONTENTS

LIST OF FIGURES

LIST OF TABLES

ABBREVIATIONS

α-AAA	α-aminoadipic acid
α-ASA	α-aminoadipate-δ-semialdehyde
BCIP	5-bromo-4-chloro-3-indoyl phosphate *p*-toluidine salt
BSA	bovine serum albumin
BTP	bis tris propane
CNS	central nervous system
Δ^1-P2C	Δ^1-piperideine-2-carboxylic acid
Δ^1-P6C	Δ^1-piperideine-6-carboxylic acid
D-AAO	D-amino acid oxidase
DCPIP	dichlorophenol indophenol
ddH_2O	double deionized water
DMF	dimethyl formamide
EDTA	ethylenediaminetetraacetic acid
EGTA	ethylene glycol-bis(β-aminoethyl ether) N,N,N',N'-tetraacetic acid
FAD	flavin adenine dinucleotide
FMOC	9-fluorenylmethyl chloroformate
GABA	γ-aminobutyric acid
HEPES	N-[2-hydroxyethyl]piperazine-N'-[2-ethanesulfonic acid

ABBREVIATIONS (Cont.)

HPLC	high performance liquid chromatography
L-PA	L-pipecolic acid
L-PADH	L-pipecolic acid dehydrogenase
L-PO	L-pipecolic acid oxidase
LSC	liquid scintillation counter
MES	N-[2-hydroxyethyl]piperazine-N'-[2-hydroxypropanesulfonic acid
NAD^+	nicotinamide adenine dinucleotide
$NADP^+$	nicotinamide adenine dinucleotide phosphate
NBT	*p*-nitro blue tetrazolium chloride
PES	phenazine ethosulfate
PITC	phenylisothiocyanate
PMS	phenazine methosulfate
PMSF	phenylmethylsulfonyl fluoride
SDS	sodium dodecyl sulfate
SDS-PAGE	sodium dodecyl sulfate-polyacrylamide gel electrophoresis
TFA	trifluoroacetic acid
TLC	thin layer chromatography
V_e	elution volume
V_o	void volume

PARTIAL PURIFICATION AND CHARACTERIZATION OF L-PIPECOLIC ACID DEHYDROGENASE FROM RABBIT KIDNEY CORTEX

CHAPTER I

BACKGROUND

DISCOVERY OF L-PIPECOLIC ACID

L-Pipecolic acid (L-PA), 2-carboxypiperidine (Figure I.1), was first isolated from the non-protein nitrogenous fractions of *Phaseolus vulgarius*.[1] L-PA has been found extensively in leguminous plants such as green beans and clover as well as apples and hops.[2-5] Chromatographic fractions from extracts of wheat flour and certain algae groups were also found to contain L-PA.[6,7]

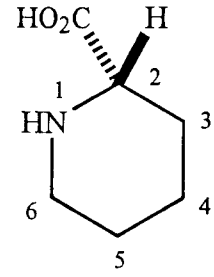

Figure I.1 Structure of L-pipecolic acid (L-PA).

As L-PA became recognized as a prominent biochemical constituent in many plant species, investigations on the origin and metabolic relationships of L-PA became important. The highest levels of L-PA were found concentrated in the seeds of plants and it was suggested that L-PA may serve as a reserve form of nitrogen.[8] The origin of L-PA was elucidated by supplying [6-^{14}C]-lysine to *P. vulgarius* and discovering the L-PA subsequently extracted contained radioactivity.[8] It was concluded from this experiment that L-PA also functions as an intermediate in the degradation of lysine.

LYSINE BIOSYNTHESIS

Lysine is an essential amino acid for many animal species and is therefore required in the diet. Two pathways for the biosynthesis of L-lysine exist. Green plants and bacteria synthesize L-lysine from L-aspartate via the diaminopimelate pathway (Scheme I.1).[9] The number of reactions involved in the conversion of L-aspartate to *meso*-diaminopimelate is species dependent. Decarboxylation of *meso*-diaminopimelate by diaminopimelate decarboxylase yields L-lysine.

L-Lysine biosynthesis in bacteria and plants:

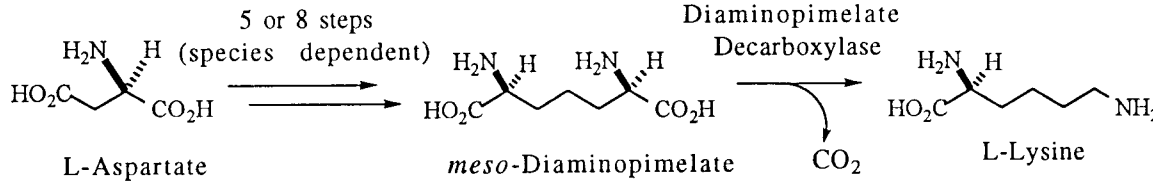

Scheme I.1

In lower eukaryotes, e.g., yeast and fungi, L-lysine is synthesized via the α-aminoadipate pathway (Scheme I.2).[10] L-Saccharopine is the key intermediate of this pathway and is produced by the condensation of L-α-aminoadipate-δ-semialdehyde (α-ASA) and L-glutamate. L-Saccharopine is oxidized to L-lysine in a nicotinamide adenine dinucleotide (NAD^+)-dependent reaction catalyzed by saccharopine dehydrogenase.

DEGRADATION OF LYSINE

Two pathways have evolved for the degradation of lysine in mammals and these are diagrammed in Scheme I.3. Initially, Rothstein and Miller proposed that L-PA was an intermediate in the major pathway for lysine degradation.[11] In support of this theory, rats that were injected with radiolabeled lysine were found to excrete radiolabeled L-PA.[11] This hypothesis was further strengthened by evidence that the α-amino group of lysine

L-Lysine biosynthesis in yeast and fungi:

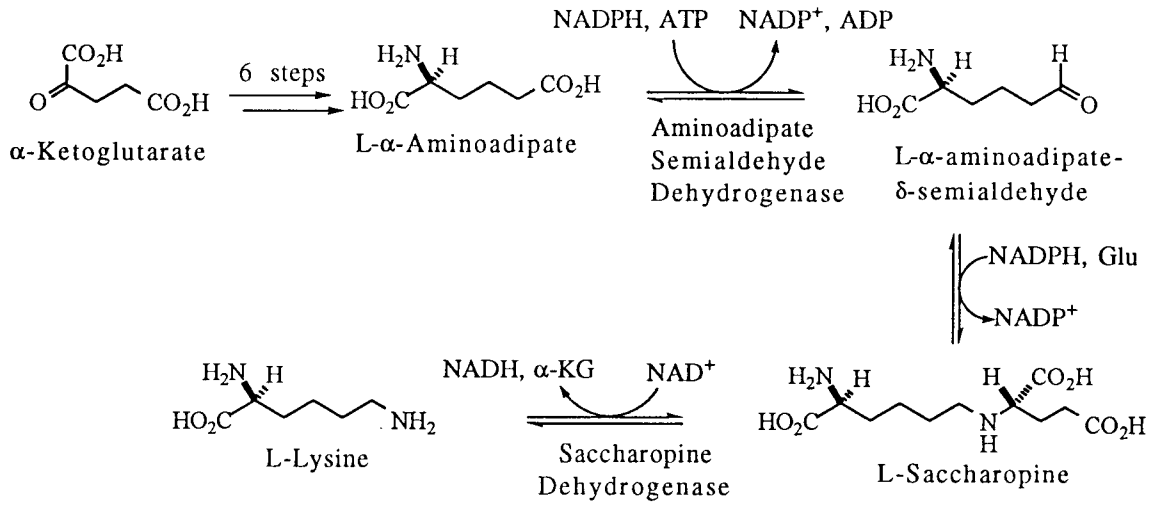

Scheme I.2

was lost during the degradation process.[12] The removal of the α-amino group was not consistent with a saccharopine intermediate (Scheme I.2).

In later studies, Higashino and coworkers incubated uniformly labeled L-[^{14}C]-lysine with rat liver homogenates and discovered that α-ketoglutarate was required for the emission of $^{14}CO_2$.[13] Furthermore, labeled saccharopine was detected indicating that the saccharopine pathway is operational during L-lysine degradation. Additional studies in rabbits provided further proof of the importance of the saccharopine pathway. In rabbits the production of $^{14}CO_2$ from L-[^{14}C]-lysine was reduced by the addition of L-α-aminoadipate (α-AAA), but not L-PA.[14] The negligible effect of L-PA on the reduction of $^{14}CO_2$ emission indicated that L-PA was not an intermediate in L-lysine degradation. It was thus concluded that the primary route of L-lysine degradation occurred via saccharopine.[14] In humans, dogs and mice the saccharopine pathway has been determined to be the predominant route of L-lysine metabolism.[15-17] It is interesting to note that the major degradation pathway of lysine in animals is the reversal of the L-α-aminoadipate biosynthetic pathway found in yeast in fungi.[18,19]

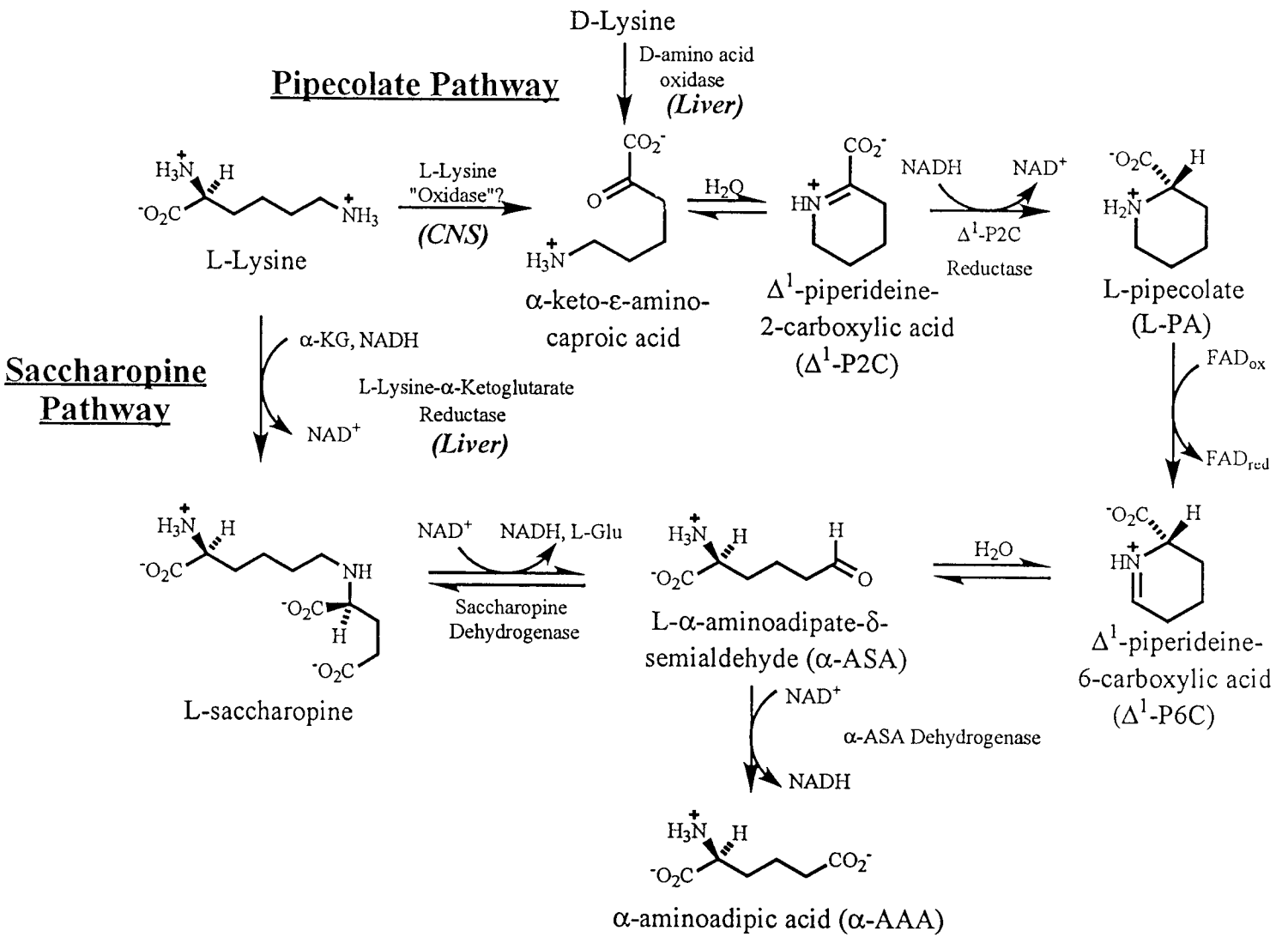
D-Lysine
D-amino acid oxidase
(Liver)
Pipecolate Pathway
L-Lysine
L-Lysine "Oxidase"?
(CNS)
α-keto-ε-amino-caproic acid
H2O
Δ1-piperideine-2-carboxylic acid (Δ1-P2C)
NADH
NAD+
Δ1-P2C Reductase
L-pipecolate (L-PA)
FADox
FADred
Saccharopine Pathway
α-KG, NADH
NAD+
L-Lysine-α-Ketoglutarate Reductase
(Liver)
L-saccharopine
NAD+
NADH, L-Glu
Saccharopine Dehydrogenase
L-α-aminoadipate-δ-semialdehyde (α-ASA)
H2O
Δ1-piperideine-6-carboxylic acid (Δ1-P6C)
NAD+
α-ASA Dehydrogenase
NADH
α-aminoadipic acid (α-AAA)

Scheme I.3

L-PIPECOLIC ACID PATHWAY

Although the L-PA pathway was not found to be the major route of L-lysine degradation, it was important to determine what role the L-PA pathway plays in lysine degradation. To elucidate the pathway further, Grove and Henderson incubated rat liver homogenates with D-[$^{14}C_6$]-lysine and subsequently detected high levels (40% of the total radioactivity) of radiolabeled L-PA whereas α-AAA was detected at much lower levels (0.02% of the total radioactivity).[20] Incubation of the liver homogenate with L-[$^{14}C_6$]-lysine did not produce radiolabeled L-PA. Further investigation revealed that the removal of the α-amino group only occurred in the conversion of D-lysine to L-PA and it was concluded that the production of L-PA in the liver occurred by the degradation of D-lysine.[21]

Even though the conversion of D-lysine to L-PA was documented in rat liver, the intermediates of the pathway had not been characterized. The conversion of D- and L-lysine to α-keto-ε-aminocaproic acid rather than α-ASA was elucidated using specifically labeled ^{15}N lysine.[21] Furthermore, D-amino acid oxidase had been detected in liver and shown to convert D-lysine to α-keto-ε-aminocaproic acid.[22] It was also demonstrated that α-keto-ε-aminocaproic acid was in equilibrium with the cyclic imine form, Δ^1-piperideine-2-carboxylic acid (Δ^1-P2C).[23] Finally, Δ^1-P2C was stereospecifically reduced by a NADH-dependent reductase producing L-PA.[24]

Even though L-lysine is primarily degraded through the saccharopine pathway in the liver, it is interesting to note that in the brain the saccharopine pathway enzymes are not detected.[25,26] Instead, L-lysine has been shown to be degraded to L-PA in the brain.[27] These studies suggest that the L-PA pathway is the major route of L-lysine degradation in the central nervous system (CNS).[28] The conversion of L-lysine to α-keto-ε-aminocaproic acid has been indicated by the detection of Δ^1-P2C, however, the enzyme in the CNS responsible for this conversion has not been isolated.[24]

The formation of L-PA was demonstrated in the liver and brain, however the intermediates in the degradation of L-PA to α-AAA had not been identified. In the 1960's Rodwell and coworkers examined pipecolic acid metabolism in the soil microorganism *Pseudomonas putida*. Studies of L-PA metabolism were carried out in *P. putida* because L-PA could be supplied as the sole source of carbon and nitrogen.[29] The oxidation of L-PA by *P. putida* resulted in the formation of α-AAA, suggesting a close similarity to the pathway postulated for the mammalian system. Studies on *P. putida* grown in the presence of L-PA and bisulfite resulted in the isolation of two new compounds, Δ^1-piperideine-6-carboxylic acid (Δ^1-P6C) and α-ASA.[30] It was suggested

that Δ^1-P6C and α-ASA were intermediates in the conversion of L-PA to α-AAA. Further investigation showed that α-AAA was subsequently converted to glutamate.[31]

The enzyme required for the oxidation of L-PA to Δ^1-P6C in *P. putida* was isolated and partially characterized. The protein was shown to be a flavin-requiring membrane-bound dehydrogenase associated with electron transport components.[32] The enzyme involved in the conversion of α-ASA to α-AAA, the second step in the degradation of L-PA, was shown to be nicotinamide adenine dinucleotide phosphate ($NADP^+$)-dependent.[33] These observations support the L-PA degradation pathway shown in Scheme I.3.

PHARMACOLOGICAL ROLE OF L-PIPECOLIC ACID

Lysine is metabolized specifically to L-PA in the brain of humans, dogs, rats, mice and chicks.[27,28,34,35] Because the L-PA pathway is the major pathway for the degradation of lysine in the CNS, the potential neurological significance of L-PA was studied. L-PA has been shown to have a neuromodulatory role on GABAergic neurotransmission.[36] Elevated levels of L-PA have also been associated with Zellweger syndrome and familial hyperlysinemia, both of which are associated with severe cerebral dysfunction.[37-39] Further study of the enzymes involved in the L-PA pathway may provide insight into the role of L-PA in these diseases.

L-PIPECOLIC ACID OXIDATION

The specialized role of L-PA metabolism in many organisms spurred further investigation of the pathway. The oxidation of L-PA has been investigated in a variety of species. In the bacterium, *P. putida*, the oxidation of L-PA to α-ASA is catalyzed by a flavin adenine dinucleotide (FAD) requiring membrane-bound dehydrogenase associated with an electron transport particle.[32] In the lower eukaryote *Rhodotorula glutinis*, a red yeast, L-PA is metabolized by a soluble oxidase which requires molecular oxygen and produces H_2O_2.[40] This enzyme has been partially purified and reported to require no external cofactor, and was suggested to be linked to an internal electron exchange system.[40,41] In *Neurospora crassa*, L-PA oxidation is predicted by the observed conversion of D-lysine to L-lysine via L-PA (Scheme I.4).[42]

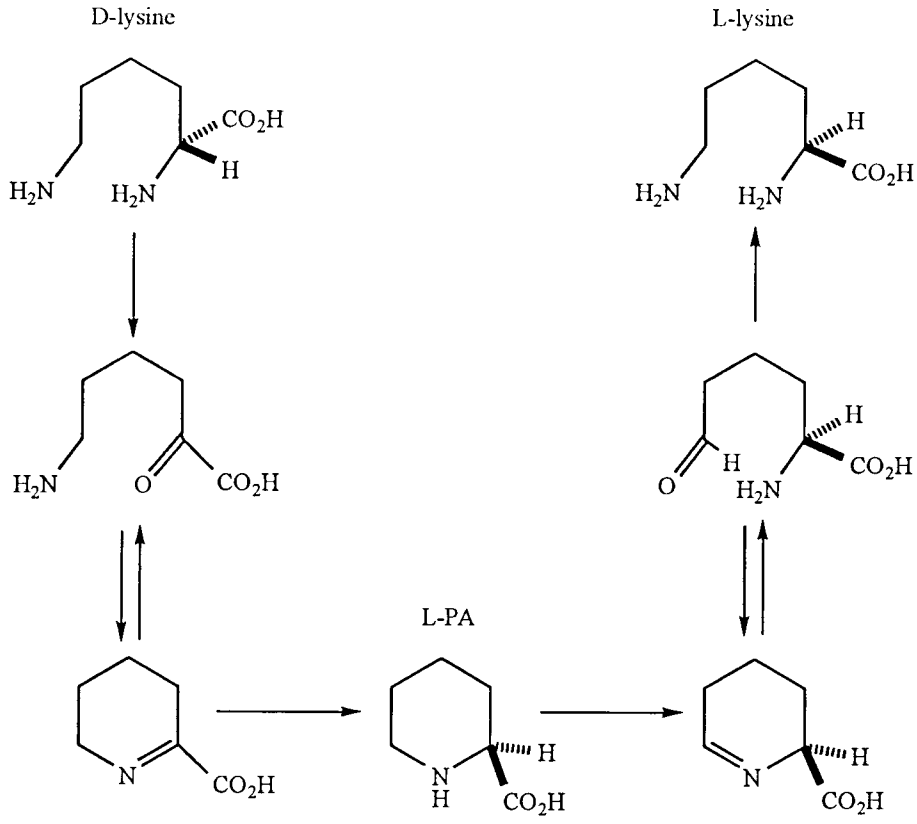

Scheme I.4

This same pathway is thought to operate in the green plant *Nicotiana glauca* based on similar observations.[43,44] These diverse organisms serve as useful comparative models for detailed studies of L-PA oxidation in mammalian systems.

Early studies on the oxidation of L-PA were conducted in rats, an animal which excretes, rather than degrades, L-PA.[16] This animal model chosen for these studies may explain the early lack of information on the L-PA pathway in mammals. Later investigations on the subcellular metabolism of L-PA was carried out on nine species of mammals as summarized in Table I.1.[45-49] L-PA oxidation was localized in the mitochondria in the rabbit, guinea pig, dog, pig and sheep.[46] Initially no L-PA oxidation was detected in the rat and mouse.[46] A more sensitive assay was developed and it was shown in rats that L-PA was degraded in the mitochondria and peroxisomes.[50] In primates L-PA was oxidized in the peroxisomes.[47,48]

Table I.1 Organellular location of L-PA oxidation in mammals.

Species	Mitochondria	Peroxisomes
Rabbit	+	
Guinea Pig	+	
Dog	+	
Pig	+	
Sheep	+	
Monkey		+
Human		+
Mouse	-	-
Rat	+	+

Further investigation lead to the discovery that the highest level of L-PA oxidation was in the mitochondria of rabbit kidney cortex and peroxisomes of monkey liver.[45] A comparison of the mitochondrial and peroxisomal metabolism of L-PA was conducted in the rabbit and cynomolgus monkey and is summarized in Table I.2.[45]

Table I.2 Comparison of rabbit and monkey metabolism of L-PA.

Characteristic	Rabbit	Monkey
Tissue with highest activity	Kidney Cortex	Liver
Subcellular location	Mitochondria	Peroxisomes
Reaction product detected	α-Aminoadipic Acid	α-Aminoadipic Acid
Specificity	L-Pipecolic Acid	L-Pipecolic Acid
K_m^{app}	0.74 mM	4.22 mM
Effect of:		
FAD	Enhances	None
PES	Enhances	Inhibits
Antimycin A	Inhibits	None

The final product of L-PA degradation detected in both tissue preparations was α-AAA. In both the rabbit and the monkey the oxidative activity was highly specific for L-PA, however the monkey preparation exhibited a six fold higher K_m for the substrate.

The addition of FAD and an artificial electron acceptor, phenazine ethosulfate (PES), enhanced the activity in the rabbit preparation. The activity from the rabbit preparation was inhibited by antimycin A, an electron transport chain inhibitor. This suggests that the electrons from the oxidation of L-PA are eventually shuttled to the electron transport chain and is consistent with the location of the enzyme in the mitochondria.

Recently, the primate enzyme catalyzing the oxidation of L-PA was isolated and characterized from Rhesus monkey liver.[47] L-pipecolic acid oxidase (L-PO) was shown to be a peroxisomal membrane-associated monomer with a molecular weight of 46 kDa, a pI of 8.9 and to contain a covalently bound flavin exhibiting absorption maxima at 457 and 383 nm with a shoulder at 480 nm.

Little is known about the mitochondrial dehydrogenase from any of the previously mentioned sources. The following chapters describe progress toward the purification and characterization of L-pipecolic acid dehydrogenase (L-PADH) from rabbit kidney cortex.

CHAPTER II

PARTIAL PURIFICATION AND CHARACTERIZATION OF L-PIPECOLIC ACID DEHYDROGENASE

INTRODUCTION

Chapter I discussed the similarities and differences of the various known enzymes involved in the oxidation of L-pipecolic acid. Among mammals, the organellular location of L-PA oxidation was shown to be species dependent.[46] The primate enzyme responsible for the oxidation of L-PA was determined to be a membrane-associated peroxisomal oxidase possessing a covalent flavin and producing H_2O_2.[45,47] Initial studies by Mihalik and Rhead revealed that in lower mammals the enzyme was a soluble mitochondrial dehydrogenase requiring a flavin cofactor as well as an artificial electron acceptor. [45]

The peroxisomal oxidase has been purified and characterized from Rhesus monkey liver.[47] L-Pipecolic acid oxidase (L-PO) was determined to be a 46 kDa monomer, with a pH optimum of 8.5, a pI at 8.9 and a K_m of 3.7 mM with a V_{max} of 2.1 $\mu mol \cdot min^{-1} \cdot mg^{-1}$ for the natural substrate, L-PA. The mitochondrial dehydrogenase has not been isolated from any mammalian source and the one of the goals of this project was to purify to homogeneity and fully characterize the enzyme. This chapter describes the partial purification and characterization of L-pipecolic acid dehydrogenase from rabbit kidney cortex.

MATERIALS AND METHODS

Materials. All biochemicals were purchased from Sigma, Fisher or VWR. All buffers and solutions were prepared using double deionized (NANOpure, Barnstead) and filtered (0.45 μm) water. D,L-[2,3,4,5,6-^{3}H]-pipecolic acid was custom synthesized by Amersham. Sodium boro[^{3}H]hydride was purchased form Dupont NEN. UniverSol scintillation cocktail was purchased from ICN. Radioactivity was detected on a Beckman LS 6000SC or a Beckman LS 6800 liquid scinitillation counter. Frozen rabbit kidney cortexes were obtained from Pel-Freez Biologicals. DEAE Fast Flow, butyl, octyl and

phenyl Sepharose® was purchased from Pharmacia. Dowex 50W-X8 (100-200 mesh, H^+ form), gel filtration standards, protein A Sepharose®, Sephadex® G-150, G-100 and G-75 were from Sigma. Acrylamide, gel silverstaining kit, goat anti-rabbit IgG, hydroxylapatite, AG 1X (100-200 mesh, acetate form), Mono S and Mono Q column chromatography resins were obtained from BioRad. Toyopearl® phenyl and ether resins were purchased from TosoHaas. The perfusion chromatography resins, polyethyleneimine (PI) and phenyl (HP2), were from PerSeptive Biosystems. Perfusion chromatography analysis by HPLC was carried out on a Beckman BioSys 510 System. Spectrophotometric studies were performed using a Hitachi U2000 spectrophotometer. DEAE-cellulose chromatography resin, silica gel and reverse phase (C_{18}) thin layer chromatography (TLC) plates were purchased from Whatman. HPLC analysis was carried out on a Beckman System Gold System using a 4.6 x 100 mm (3 μ) reverse phase (C_{18}) column (Microsorb MV, Rainin). Dialysis cartridges were obtained from Pierce. The antisera for the primate oxidase was a gift from Prof. Stephanie J. Mihalik (Johns Hopkins University).

L-[2,3,4,5,6-3H]-Pipecolic acid: 2-Pyridinecarboxylic acid was catalytically reduced with tritium gas by Amersham. The resulting D,L-[2,3,4,5,6-^{3}H]-pipecolic acid (D,L-[^{3}H]-PA) had a specific activity of 6200 mCi/mmol and was separated from its radiolytic degradation products and converted to the homochiral L-form by the method of Mihalik and Rhead.[45] D,L-[^{3}H]-PA (7 mCi) was applied to a sequential anion exchange - cation exchange chromatography system in which the upper column consisted of 1 mL (0.5 x 5 cm) of AG1-X8 anion exchange resin and the lower column consisted of 20 mL (1.5 x 11 cm) Dowex 50W-X8 cation exchange resin.[45] Both columns were washed with 55 mL ddH_2O, until no further radioactivity was eluted. The cation exchange column was washed with 80 mL of 0.5 N HCl and then the D,L-[^{3}H]-PA was eluted with 2 N HCl. Fractions containing radioactivity were pooled and concentrated to dryness on a rotary evaporator. The residue was resuspended in 10 mL of ddH_2O and brought to pH 6 with 6 M NH_4OH. The material was then applied to a 110 mL (2.5 x 22 cm) Dowex 50W-X8 column and washed with 250 mL of ddH_2O. The D,L-[^{3}H]-PA was eluted with 1 M NH_4OH and concentrated to dryness. The solid was resuspended in 10 mL of ddH_2O and then dried again. This process was repeated five additional times for a total of six washes. The purified D,L-[^{3}H]-PA was dissolved in 3 mL of 0.1 M sodium phosphate buffer, pH 8.0, and brought to a specific activity of 500 μCi/μmol with unlabeled L-pipecolic acid. After adding 4.8 units of D-amino acid oxidase (D-AAO) and 7.4 mM $NaBH_4$, the reaction was stirred at 37 °C for one hour, at which time the same amounts of D-AAO and $NaBH_4$ were added and the reaction continued for another two hours. The

reaction converts the D-enantiomer to the L-enantiomer by stereospecifically oxidizing D-PA to Δ^1-piperideine-2-carboxylate (Δ^1-P2C) while L-PA is unaffected. The Δ^1-P2C is then reduced with $NaBH_4$ to form D,L-[^{3}H]-pipecolic acid. By continuously repeating the oxidation and reduction cycle, D-PA can be quantitatively converted to L-PA.[51] L-[^{3}H]-Pipecolic acid is separated from the reaction mixture using an 85 mL (2.5 x 17 cm) Dowex 50W-X8 cation exchange column. After washing the column with 135 mL of ddH_2O, the L-[^{3}H]-PA was eluted with 1 M NH_4OH, concentrated to dryness, and was subsequently washed with 10 mL of ddH_2O. The conversion of D,L-[^{3}H]-PA to L-[^{3}H]-PA was checked for completeness by incubating 0.5 units of D-AAO with 1 µL of the converted L-[^{3}H]-PA mixture (0.8 mM) in 0.1 M sodium phosphate, pH 8.0, along with 8,000 units of catalase. If any significant amount of the D-enantiomer was present, the release of ^{3}HOH should be observed. No ^{3}HOH was detected when the D-AAO reaction mixture was applied to a cation exchange column and the unretained fraction was analyzed for radioactivity. L-[^{3}H]-Pipecolic acid was stored at -86 °C at a concentration of 10 mM and a specific activity of 500 µCi/µmol.

Enzyme assay. The enzymatic oxidation of L-pipecolic acid was measured through the release of ^{3}HOH from L-[2,3,4,5,6-^{3}H]-pipecolic acid (L-[^{3}H]-PA).[45] Fifteen µL aliquots of the enzyme fractions were incubated for one hour at 37 °C in an assay mixture containing 12 mM Tris, 5 mM KCl, 0.1 mM FAD, 1.0 mM PES, and 62.5 µM L-[^{3}H]-PA (125 µCi/µmol) at pH 8.5 in a total volume of 60 µL. The reaction was halted by placing the tubes on ice. The assay mixture was applied to a Dowex 50W-X8 cation exchange column (0.8 mL) and the column was washed with 4.5 mL of ddH_2O. The collected water was mixed with 10 mL of scintillation cocktail and the radioactivity was measured in a liquid scintillation counter (LSC).

Protein dependence. L-PADH was incubated at 37 °C in the above assay mixture at final protein concentrations of 7.8, 5.2 and 2.6 mg/mL. For each of the three different protein concentrations duplicate assays were performed and the amount of ^{3}HOH produced was measured at 15, 30 and 45 minutes.

Effect of unlabeled L-PA on radioassay. 90 µg of L-PADH was incubated at 37 °C in assay mixtures containing 12 mM Tris, 5 mM KCl, 0.1 mM FAD, 1.0 mM PES with final concentrations of L-PA of 64 µM (125 µCi/µmol), 320 µM (25 µCi/µmol), and 640 µM (12.5 µCi/µmol). For each of the different L-PA concentrations duplicate assays were conducted and the amount of released ^{3}HOH was measured at 15, 30, 45 and 60 minutes.

pH Dependence. Fifteen µL aliquots of an active L-PADH fraction from a Sephadex® G-150 column were incubated for one hour at 37 °C in 25 mM buffer

(morpholinoethanesulfonic acid (MES), bis tris propane (BTP), and potassium carbonate) at various pH values along with 0.1 mM FAD, 1.0 mM PES, and 62.5 μM L-[^{3}H]-PA (125 μCi/μmol) in a total volume of 60 μL. The reactions were halted by placing the reactions on ice and the amount of ^{3}HOH produced was determined as described above.

Partial purification. All steps were carried out at 4 °C unless otherwise specified. In a typical preparation 100 g of frozen, mature rabbit kidney cortexes were partially thawed and finely minced with a razor blade. The tissue was added to 200 mL of preparation buffer (10 mM KCl, 50 mM *N*-(2-hydroxyethyl)piperazine-*N'*-ethanesulfonic acid (HEPES), pH 7.4, 0.1 mM ethylenebis(oxyethylenenitrilo)tetraacetic acid (EGTA), and 0.1 mM phenylmethylsulfonyl fluoride (PMSF)) and the slurry was homogenized by two passes with a Potter-Elvehjem homogenizer. The homogenate was centrifuged at 800 x g for 10 minutes and the supernatant decanted and centrifuged at 27,000 x g for 30 minutes. The pellet was discarded and the cell free supernatant was applied at a rate of 2 mL/min to a DEAE-cellulose column (5 x 8 cm) equilibrated in 10 mM KCl, 50 mM HEPES, pH 7.4, and 0.1 mM EGTA. The column was washed with the equilibration buffer and bound protein was eluted at 2 mL/min using a step gradient of increasing concentration of KCl in 50 mM HEPES, pH 7.4, 0.1 mM EGTA. Fractions were assayed for L-PADH activity which typically eluted between 75 mM and 150 mM KCl. The active fractions were pooled and subjected to ammonium sulfate precipitation by the slow addition of ammonium sulfate to 45% saturation. The solution was allowed to equilibrate for 30 minutes while stirring and then centrifuged at 27,000 x g for 30 minutes. The resulting pellet was suspended in a minimal amount of 250 mM KCl, 50 mM potassium phosphate, pH 7.4, 10% glycerol. This material was chromatographed on a Sephadex® G-150 size exclusion column (2.5 x 110 cm) equilibrated in 250 mM KCl, 50 mM potassium phosphate, pH 7.4, at a flow rate of 0.4 mL/min. L-PADH activity began eluting after 350 mL. The active fractions were pooled and adjusted to 1 M ammonium sulfate. This material was applied to a butyl Sepharose® column (1.5 x 3 cm) equilibrated in 1 M ammonium sulfate, 50 mM HEPES, pH 7.4, at a flow rate of 1 mL/min. Using a step gradient, the highest specific activity of L-PADH eluted between 0.75 M and 0.5 M ammonium sulfate. Fractions containing high L-PADH activity were pooled and concentrated by centrifugation (5,000 x g) using an Amicon Centriprep ultrafiltration device with a 10 kDa molecular weight cutoff. The concentrated sample (2 mL) was then dialyzed overnight against a low salt buffer (500 mL of 10 mM KCl, 50 mM HEPES, pH 7.4), using a dialysis cartridge with a molecular weight cutoff of 10 kDa. The dialysate was applied to a DEAE Fast Flow column (1.5 x 2.5 cm), equilibrated in dialysis buffer, at a rate of 3 mL/min. The column was washed with dialysis buffer and bound protein

was eluted using a linear gradient of increasing KCl concentration from 10 mM to 200 mM. The active fractions were pooled and concentrated by ultrafiltration.

Protein concentration. During purification, protein quantification was determined by the method of Bradford.[52] A standard curve was produced by using known concentrations of BSA at 0, 0.1, 0.375, 0.50, 0.75, and 1.0 mg/mL.

SDS-PAGE analysis. Sodium dodecylsulfate-polyacrylamide gel electrophoresis (SDS-PAGE) analyses were carried out using a BioRad Mini-Protean II system. Buffers for a 12.5% resolving gel and a 4% stacking gel were based on the method of Laemmli.[53] SDS-PAGE sample loading buffer contained 62.5 mM Tris, pH 6.8, 10% glycerol, 2% SDS, 15% β-mercaptoethanol and 0.005% bromophenol blue. Tank buffer consisted of 5 mM Tris, pH 8.3, 38 mM glycine and 0.02% SDS. Denaturing gels were run at constant voltages of 100 V through the stacking gel and 200 V through the resolving gel.

Gel staining. Gels were stained in 3 mM Coomassie brilliant blue R, 40% MeOH, and 10% HOAc. Protein bands were visualized by destaining in an aqueous solution containing 40% MeOH and 10% HOAc. Silver stained gels were developed using the silver staining kit from BioRad.

Mitochondria isolation.[54] Frozen rabbit kidney cortexes (25 g) were finely minced and homogenized in 75 mL of 250 mM sucrose, 6.8 mM HEPES, pH 7.5, 0.1 mM EGTA. The slurry was centrifuged at 3,200 x g for one minute, the supernatant decanted and centrifuged for two minutes at 17,000 x g. The pellets were washed with the same buffer and centrifuged for 4.5 minutes at 19,000 x g. The floculent pellets were resuspended in homogenizing buffer and exposed to a freeze/thaw procedure to break open the mitochondrial membrane. The mixture was rapidly frozen by submersion into a dry ice and acetone bath and then rapidly thawed in a 37 °C H_2O bath. This technique was repeated several times. The mixture was centrifuged at 45,000 x g for one hour. The resultant supernatant and pellet were assayed for glutamate dehydrogenase activity.

Glutamate dehydrogenase assay.[54] The assay mixture contained 50 mM potassium phosphate, pH 8.0, 0.12 mM NAD^+, and 30 mM potassium glutarate. The reduction of NAD^+ was monitored at 340 nm. L-Glutamate dehydrogenase purchased from Sigma was used as a standard.

Native molecular weight. A 160 mL Sephadex® G-100 column (1.5 x 90 cm) was calibrated according to the manufacturers directions in 50 mM potassium phosphate, pH 7.4, 250 mM KCl, at a flow rate of 0.33 mL/min. Blue dextran was used to determine the void volume (V_0) of the column. The molecular weight standards included bovine serum albumin, alcohol dehydrogenase, carbonic anhydrase, β-amylase and cytochrome C. Each sample mixture was loaded in a 2 mL volume containing 50 mM potassium phosphate,

pH 7.4, 250 mM KCl, 5% glycerol and the elution volumes (V_e) were measured at the point where the UV absorbance (280 nm) was greatest. The log of the molecular weight was plotted versus the ratio of the elution volume and the void volume. A calibrated Sephadex® G-75 column was also used to estimate the native molecular weight using the same buffer and a flow rate of 0.2 mL/min. Blue dextran was used to measure V_0 and four molecular weight standards were applied in 2 mL of the same loading buffer. The molecular weight standards included bovine serum albumin, cytochrome C, carbonic anhydrase and aprotinin. A sample of partially purified L-PADH (1.5 mg) was analyzed on each column and the V_e was measured at the point where the specific activity was highest.

Native gel electrophoresis: Native gel electrophoresis was carried out following the procedure of Ornstein and Davis.[55,56] Slab gels were run using a BioRad Mini-Protean II system. The gel buffer was comprised of 0.5 M Tris, pH 6.8, for the 4% stacking gel, and 1.5 M Tris, pH 8.8, for the 6% and 10% resolving gels. The tank buffer contained 25 mM Tris, pH 8.8, 192 mM glycine, and the sample loading buffer contained 32 mM Tris, pH 6.8, 5% glycerol and 0.005% bromophenol blue.

The Jovin buffer system was also tried.[57] The Jovin system is a discontinuous system in which the cathode buffer was comprised of 50 mM HCl and 63 mM bis tris, pH 7.4, and the anode buffer contained 44 mM TES and 110 mM bis tris, pH 7.25. The gel buffer contained 0.5 M BisTris, 9.22 M HCl, pH 6.6 and the sample loading buffer contained 125 mM BisTris, pH 6.61, 5% glycerol, and 0.005% of bromophenol blue.

A continuous buffer system described by McLellan in which the gel buffer is the same as the tank buffer (250 mM Tris, 125 mM boric acid, pH 8.7) was also used.[58] The sample loading buffer also contained 5% glycerol and 0.005% bromophenol blue.

All gels dimensions were 5 x 7.4 x 0.075 cm, unless otherwise indicated. Prior to loading protein samples, all native gels were run at 25 V for one hour in buffer containing sodium thioglycolate (11 mg/L) to remove any residual radical species.[59] The gels were run at 4 °C at constant voltage (25 V) for the length of time specified in the Results section. The gels were sliced horizontally and divided into sections for staining, assaying, and SDS-PAGE analysis (Scheme II.1).

The silver stained section was treated according to the BioRad silver staining kit instructions. The slices to be assayed were placed in 1.5 mL conical centrifuge tubes with 30 µL of 12 mM KCl, 5 mM HEPES, pH 8.5 and mashed with a pestle. The radiolabeled substrate and all cofactors were added and the mixture was assayed as described above. The slices to be analyzed by SDS-PAGE were incubated at 96 °C for 10 min in 30 µL of SDS-PAGE loading buffer and then the slices and any extra sample buffer were loaded

onto a 5 x 7.4 x 0.1 cm 12.5% acrylamide denaturing gel with a 4% acrylamide stacking gel. The gel was electrophoresed and silver stained as described above.

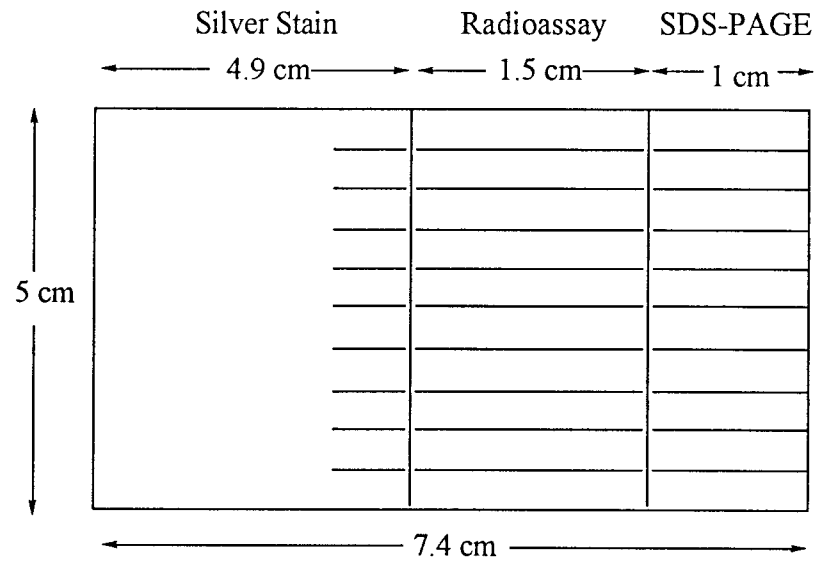

Scheme II.1

Western blot analysis. Samples of L-PADH from various purification steps were subjected to SDS-PAGE. After electrophoresis the gel was placed in transfer buffer (25 mM Tris, pH 8.5, 192 mM glycine, and 20% MeOH) for 15-30 min. The gel was then placed between a nitrocellulose membrane and filter paper and placed in a Mini Trans-Blot® (BioRad) blotting chamber containing 450 mL of transfer buffer. The protein was electroblotted to the membrane at 100 V for one hour. The membrane was washed in 50 mL of 50 mM Tris, pH 7.5, 150 mM NaCl for 10 min. Non-fat dry milk (5 g) was added to the solution which was allowed to shake for one hour. The milk mixture was decanted and the L-PO antisera (rabbit anti-monkey antisera) was added in a dilute mixture (1:2000) in 15 mL of transfer buffer with 0.05% Tween 20. The membrane was shaken in this solution overnight at 4 °C. The membrane was rinsed three times in 20 mL of transfer buffer with 0.05% Tween 20. A final rinse of 15 mL of transfer buffer with 0.3% non-fat dry milk preceded the addition of 15 μL (1:1000) of IgG antibody (goat anti-rabbit conjugated with alkaline phosphatase). The membrane was shaken in this mixture for two hours and then rinsed three times with 20 mL of transfer buffer containing 0.05%

Tween 20. The membrane was placed in 20 mL of 0.1 M Tris, pH 9.5, 0.5 mM $MgCl_2$ and the following substrates were added to visualize bands: 200 µL of *p*-nitro blue tetrazolium chloride (NBT, 30 mg/mL in 70% aqueous dimethyl formamide (DMF)) and 200 µL of 5-bromo-4-chloro-3-indoyl phosphate *p*-toluidine salt (BCIP, 15 mg/mL in DMF). Color development was stopped by rinsing the membrane with ddH_2O.

Immunoprecipitation. Initial studies were carried out on 0.5 mL fractions of partially purified L-PADH, L-pipecolate oxidase and a blank consisting of 0.5 mL of suspension buffer (10 mM KCl, 50 mM HEPES, pH 7.4). These fractions were added to 0.1 mL of protein A Sepharose® (50 mg/mL in suspension buffer) and rocked at 4 °C for one hour. The slurries were centrifuged for one minute at 3,100 x g and the supernatants were decanted into 1.5 mL conical centrifuge tubes. This initial incubation was carried out to reduce non-specific binding particles that may interact with the protein A Sepharose®. L-PO antisera (rabbit anti-monkey antisera, 3 µL) was added to the supernatants and the samples were then incubated on ice for 30 min. Protein A Sepharose® (0.1 mL of 50 mg/mL in suspension buffer) was added to each and the mixtures were rocked for 2.5 hours at 4 °C. The mixtures were centrifuged for two minutes at 3,100 x g. The supernatant was set aside and 1 mL of suspension buffer was added to the resin and centrifuged again. The supernatants from four consecutive washes were pooled. The supernatants were assayed for L-PADH activity using the radioassay. Both the resins and 20 µL of the supernatants were added to 20 µL of SDS-PAGE loading buffer. The samples were heated to 96 °C for 10 minutes. The resin mixtures were centrifuged at 5,000 x g and the resulting supernatants were analyzed on a 12.5% SDS-polyacrylamide gel, along with the aliquots of the pooled supernatant washes.

Native gel activity stain. This procedure was adapted from Witwer and Wagner.[60] L-PADH was assayed by incubating a slice from a 6% McLellan native gel in 15 mL of 0.1 M potassium phosphate buffer, pH 7.4, containing 0.1 M L-PA, 0.04 mM FAD, 0.2 mM PES, and 0.5 mM NBT at 37 °C overnight.

Isoelectric point. Isoelectrofocusing experiments were performed using a BioRad Rotofor Cell®. The Rotofor Cell® is a preparative isoelectricfocusing devise that has two different sizes of focusing chambers with membranes that divide the chambers into 20 compartments and a internal ceramic cooling finger. Rotation of the chambers at 1 rpm stabilizes against gravitational forces. Ampholytes (Biolytes, BioRad) with a pH range of 3 to 10 were used to focus L-PADH. Two different chamber sizes, one with a 60 mL capacity and one with a 20 mL capacity, were used. Run times and wattages for each experiment varied and are listed in the Results section. Glycerol (5 to 15%) was added to the samples in order to maintain the solubility of the protein. After harvesting the

protein, the pH of each fraction was tested and L-PADH activity was determined using the radioassay.

Kinetic parameters. A spectrophotometric assay was employed to determine the K_m and V_{max} values for the natural substrate, L-PA. This is a dye-linked assay which follows the reduction of dichlorophenol-indophenol (DCPIP).[61] The reaction mixture contained 12 mM Tris, pH 8.5, 5 mM KCl, 0.1 mM DCPIP (ε = 21.5 L•mmol^{-1}•cm^{-1}), 1 mM KCN, 0.07 mM FAD, 0.7 mM PES, and 25 µL of partially purified L-PADH (62 µg) in a total volume of 0.5 mL. The reaction was initiated with substrate and the reaction was monitored at 37 °C as a decrease in absorbance at 600 nm. A blank containing all the reaction components except substrate was used in the reference cell. The software package Enzyme Kinetics, from Trinity Software, was used to analyze the data.

Stereochemical course of the oxidation of L-PA. The stereochemical course of the oxidation was studied using L-PA stereospecifically deuterated at C-6.[62] The DCPIP assay was used to monitor the rate of the reaction using L-[6*R*-^{2}H]-PA and L-[6*S*-^{2}H]-PA as substrates (1 mM final concentration).

Turn-over product characterization.

Phenylisothiocyanate: Derivatization of the turnover product from the reaction of L-PADH with L-PA was attempted using phenylisothiocyanate (PITC).[63] Authentic L-PA was derivatized first to produce a standard. L-PA (2 mmol) was mixed with buffer (12 mM Tris, pH 8.5, 5 mM KCl) and 50% pyridine. PITC (50 µL) was added and the mixture incubated at 37 °C for 30 min. After incubation, 0.5 mL of 1 N HCl was added and the mixture was placed on ice for one hour. A precipitate formed and the mixture was centrifuged for 3 min at 1,000 x g. The supernatant was set aside and the pellet was resuspended in 100 µL of 1.0 N HCl and analyzed by TLC on glass-back reverse phase plates in 1:1 0.1% TFA:CH_3CN. The plate was developed with ninhydrin. Initial incubations were carried out with L-PO as a control because the turnover product has been characterized as Δ1-P6C. L-PO was incubated overnight at 37 °C in 50 µL containing 2.5 mM KCl, 2.5 mM HEPES, pH 7.4, 0.1 mM EGTA and 11.0 mM L-PA. L-PADH was incubated overnight at 37 °C in a total assay volume of 60 µL containing 12 mM Tris, 5 mM KCl, 0.1 mM FAD, 1.0 mM PES, and 12.5 mM L-PA at pH 8.5. The solutions were brought to 50% pyridine and the derivitization procedure was carried out as described above. L-PO and L-PADH reaction product mixtures were analyzed by TLC in the aforementioned solvent system. The samples were also analyzed by reverse phase (C_{18}) HPLC (4.6 x 100 mm, Microsorb MV). The column was equilibrated and run in 7:3 0.1% TFA:CH_3CN at a rate of 1 mL/min. Peaks were detected at 270 nm.

9-Fluorenylmethyl chloroformate:[64] To prepare a standard, a 20 mM solution of L-PA was made in 50 mM potassium borate, pH 9.5. 9-Fluorenylmethyl chloroformate (FMOC) was diluted to 5 mM in acetone and was added to the L-PA solution for a final concentration of 1.3 mM. Water (1 mL) was added and the solution was immediately extracted twice with 2 mL of ether to remove the excess FMOC. The aqueous layer was concentrated to dryness and the resulting solid was dissolved in 50 μL of ddH_2O. TLC analysis was carried out on reverse phase (C_{18}) plates in 1:1 100 mM phosphoric acid:CH_3CN. L-PADH was incubated at 37 °C in 50 mM borate, 0.1 mM FAD, 1.0 mM PES, and 6.5 mM L-PA at pH 9.5 in a total volume of 120 μL. 100 μL aliquots were taken from the enzyme mixture at time 0, 0.5, 1, 2, 4, and 8 hours and placed in a 1.5 mL conical centrifugation tubes. Approximately 0.3 mL of 5 mM FMOC was added to the reaction mixture followed by 0.3 mL of ddH_2O. The solution was immediately extracted twice with 1 mL of ether and the aqueous layer was concentrated to dryness. The solid was dissolved in 50 μL of ddH_2O. Reverse phase HPLC analysis was employed using an isocratic solvent system of 1:1 100 mM phosphoric acid:CH_3CN on a Microsorb MV column (4.6 x 100 mm).

Sodium boro[^{3}H]hydride reduction:[65] L-PADH was incubated in 0.5 mL containing 12 mM Tris, 5 mM KCl, 0.1 mM FAD, 1.0 mM PES, 0.1 mM L-PA, pH 8.5, at 37 °C for 1.5 hours. At this time an additional 1.0 mM PES was added and the reaction was allowed to continue for another hour. After the incubation, 12 μL of (1 μCi/μmol) NaB^3H_4 in 0.1 N NaOH was added to the mixture and kept at room temperature for 2.5 hours. The reaction was quenched with 25 μL of 1 N HCl and incubated at room temperature for 30 min. The mixture was then applied to a dual column system where the upper column consisted of 0.8 mL of AG 1X anion exchange resin and the lower column contained 1 mL of AG 50W-X8 cation exchange resin. After the enzyme reaction mixture was added, the columns were washed with 4.5 mL of ddH_2O. The eluant was added to 10 mL of scintillation counter cocktail and assayed for radioactivity. The AG 1X column was stripped with 3 mL of 1 N HOAc and the AG 50W-X8 column was stripped with 3 mL of 1 N NH_4OH. These eluants were concentrated to dryness and resuspended in 20 μL of ddH_2O. A 2 μL aliquot of the resuspended material was mixed with 5 mL of scintillation cocktail and radioactivity measured by LSC. TLC analysis of the resuspended solid was carried out on aluminum backed silica gel in 7:3 EtOH:NH_4OH and developed with ninhydrin. Sections of the plate were cut and the silica gel was scraped off, added to 5 mL of scintillation counter cocktail, and analyzed by LSC.

Formation of α-ASA/Bisulfite adduct: This procedure was developed as an assay for L-pipecolate oxidase activity in human liver for the detection of enzyme deficiency in hyperpipecolic acidemia patients.[66] L-PADH was incubated in 120 μL containing 12 mM Tris, 5 mM KCl, pH 8.5, 0.1 mM FAD, 1.0 mM PES, 10 mM $NaHSO_3$, and 62.5 μM L-[^{3}H]-PA (125 μCi/μmol). The reaction was quenched by the addition of 15 μL of ice cold 0.5 N HCl. The mixture was then applied to a 2 mL Dowex 50W-X8 column and the column was rinsed with 4.5 mL of ddH_2O. The eluant was mixed with 10 mL of UniverSol scintillation cocktail and the radioactivity was measured by LSC. TLC analysis of the resuspended solid was carried out on aluminum backed silica gel in 7:3 EtOH:NH_4OH and developed with ninhydrin.

α-Aminoadipic acid detection: Incubations were carried out with crude cell free extracts in a reaction mixture containing 12 mM Tris, 5 mM KCl, 0.1 mM FAD, 1.0 mM PES, 1.1 mM NAD^+, 3.1 mM L-PA, and 0.1 mM L-[^{3}H]-PA (500 μCi/μmol) at pH 8.5. A dual column system was used to separate L-[^{3}H]-PA and α-[^{3}H]-AAA.[45] The AG 1X column was stripped with 3 mL of 1 N HOAc and the AG 50W-X8 column was stripped with 3 mL of 1 N NH_4OH. These eluants were concentrated to dryness and resuspended in 150 μL of ddH_2O. The resuspended solid was analyzed by paper chromatography on Whatman #1 filter paper in 7.7:2.3 EtOH:H_2O.[45] Nitrogen containing compounds were visualized with ninhydrin. After development, the paper was cut into 1 cm sections, placed in 7 mL vials with 5 mL of scintillation cocktail and radioactivity was measured by LSC.

RESULTS

L-[2,3,4,5,6-^{3}H]-Pipecolic acid: D,L-[2,3,4,5,6-^{3}H]-PA was prepared by Amersham. The racemic mixture was enzymatically converted to L-[2,3,4,5,6-^{3}H]-PA which was isolated through cation exchange chromatography.[45,51] The conversion process is shown in Scheme II.2. D-[$^3H_5$]-PA is stereospecifically oxidized to Δ^1-P2C by D-AAO while the L-enantiomer is unaffected. The Δ^1-P2C is then reduced by $NaBH_4$ to form D,L-[$^3H_5$]-PA. The continuous oxidation and reduction cycle quantitatively converts D-[$^3H_5$]-PA to L-[$^3H_5$]-PA. When D-AAO was incubated with and aliquot of the converted [$^3H_5$]-PA, no ^{3}HOH was observed, suggesting that none of the D-enantiomer was present and that the reaction had continued to completeness. After

the cation exchange chromatography and enzymatic conversion, the radiochemical yield of 500 mCi/mmol L-[$^3H_5$]-PA was 79%.

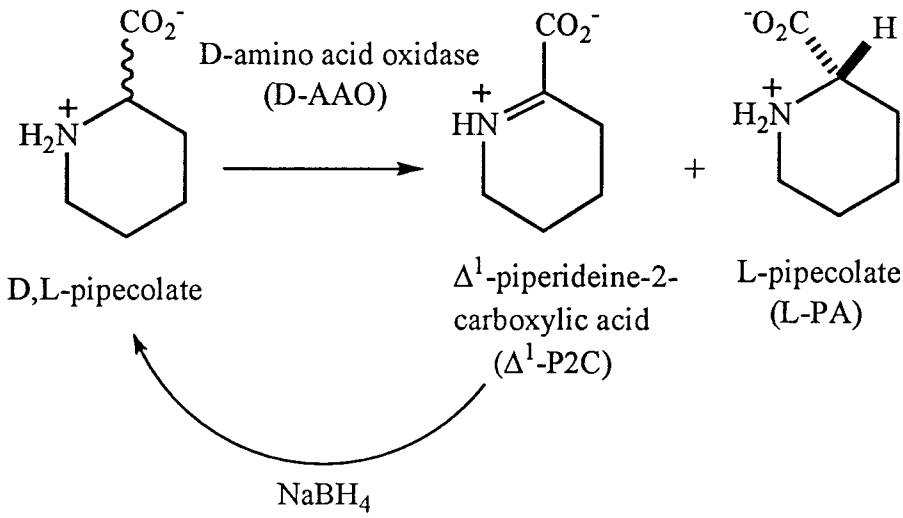

Scheme II.2

Protein Dependence. The dependence of ^3HOH production on L-PADH was measured by incubating different amounts of protein (final concentrations of 7.8, 5.2 and 2.6 mg/mL) with the assay mixture containing 12 mM Tris, 5 mM KCl, 0.1 mM FAD, 1.0 mM PES, and 62.5 μM L-[^3H]-PA (125 μCi/μmol). Figure II.1 shows the amount of tritiated water produced in the radioassay is dependent on the amount of L-PADH in the assay mixture. This indicates that the ^3HOH production is enzyme dependent, not a result of nonspecific degradation of the tritiated substrate.

Effect of unlabeled L-PA on radioassay. L-PADH was incubated in the typical radioassay mixture with different final concentrations of L-PA. The production of tritiated water was monitored by assaying the reactions at 15, 30, 46, and 60 minutes. Figure II.2 illustrates the effect of the addition of unlabeled L-PA to the radioassay reaction mixture. The resulting decrease in the amount of ^3HOH produced in proportion to added unlabeled L-PA indicates the liberated ^3HOH is produced from L-[$^3H_5$]-PA and not from a radiolabeled impurity.

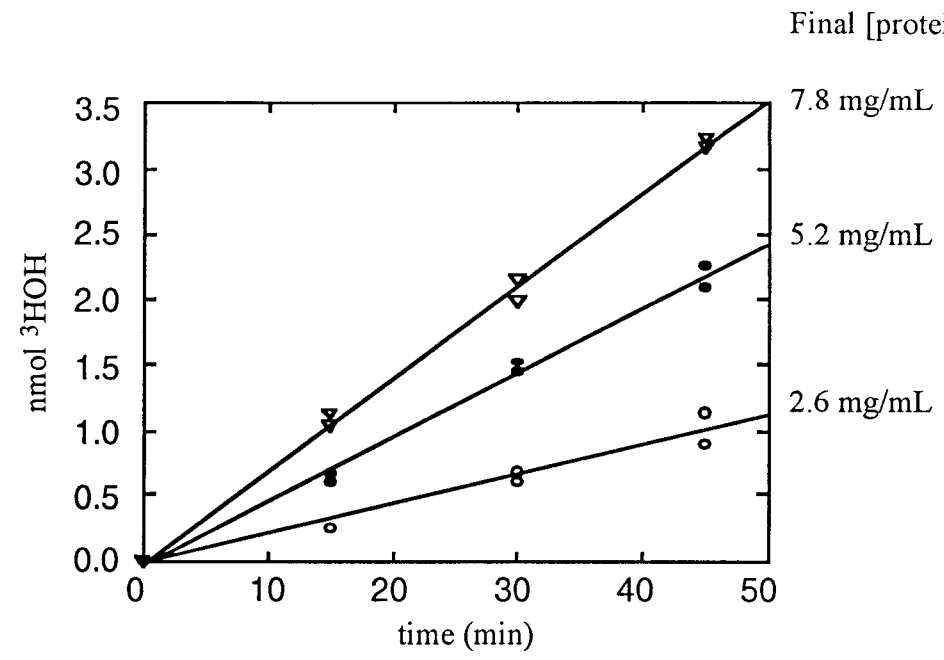

Figure II.1 Dependence of ^{3}HOH production on L-PADH concentration.

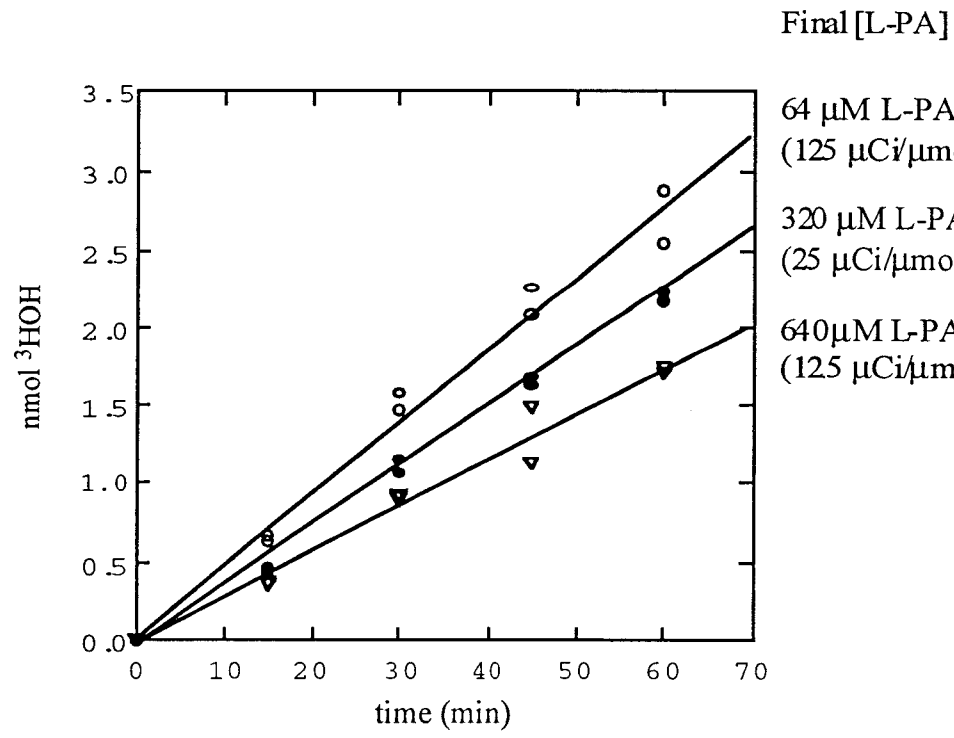

Figure II.2 Effect of unlabeled L-PA on ^{3}HOH production in the radioassay.

pH Dependence. Fractions from a size exclusion column containing L-PADH activity were used to study the pH optimum of the L-PA oxidation reaction. Samples were incubated in four different buffers at concentrations of 25 mM and various pH values as described in Materials and Methods. The highest L-PADH activity was observed at pH 8.5. Both buffers tested at this pH yielded similar results (Figure II.3).

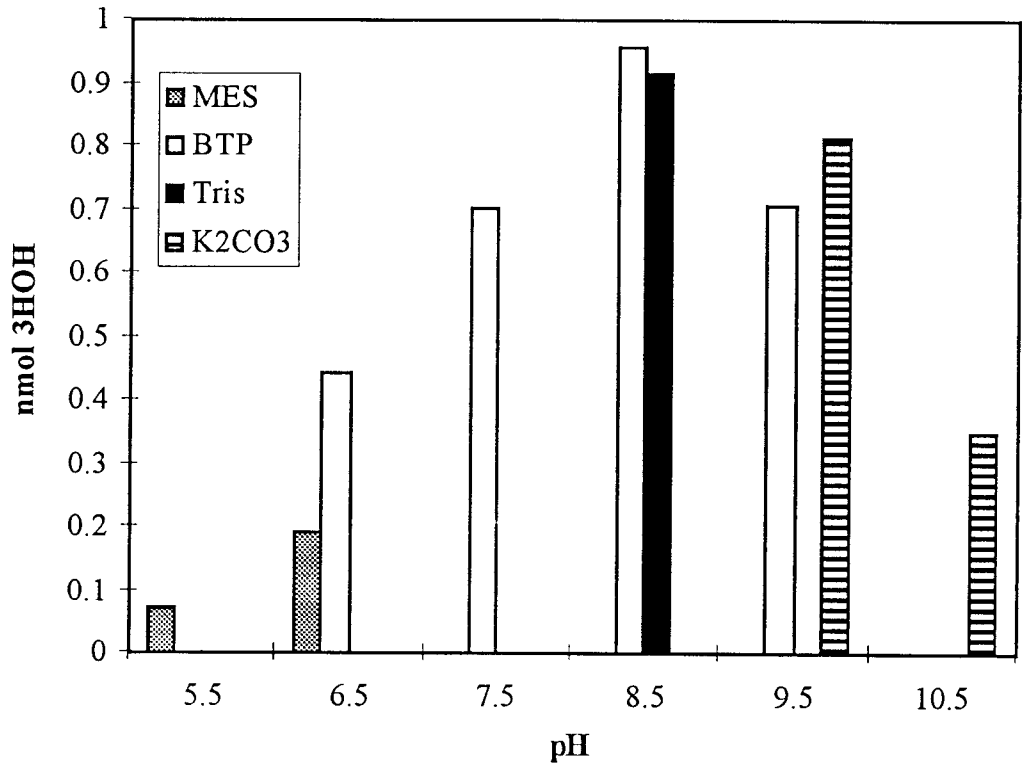

Figure II.3 pH Dependence of L-PADH.

Purification Procedure: Mature rabbit kidney cortexes were thawed, minced, homogenized and subjected to differential centrifugation as described in Materials and Methods. The pellet from the centrifugation procedure contained only 5% of the total L-PADH activity. Consequently, the supernatant was used in all further procedures. As a first step in the purification scheme, DEAE-cellulose chromatography was selected. In order to determine the optimal conditions for the column, a coarse step gradient with KCl was employed to roughly define the elution point of L-PADH. Once this broad elution

profile was determined, the procedure was repeated on a second DEAE-cellulose column using narrower steps in the KCl concentrations (Table II.1). L-PADH elutes from a DEAE-cellulose column between approximately 75 mM and 150 mM KCl thus a gradient stepping from 75 mM to 150 mM KCl was used in all future DEAE-cellulose chromatography procedures.

Table II.1 Conditions for DEAE-cellulose chromatography.

First DEAE column		Second DEAE column	
Conc. KCl	Activity (CPMs)	Conc. KCl	Activity (CPMs)
0.25 M	2849	0.05 M	0.0
0.50 M	39	0.10 M	325
0.75 M	0.0	0.15 M	1358
1.0 M	0.0	0.20 M	386
		0.25 M	129

Active fractions from the DEAE-cellulose column were pooled and subjected to 45% ammonium sulfate precipitation. Initially, precipitation experiments were carried out using the cell free supernatant. From these experiments the optimal ammonium sulfate cut was estimated to precipitate between 30% and 50% saturation (Figure II.4). Further studies with the crude material displayed the highest specific activity to precipitate between 25% and 45% saturation. When the active fraction from the DEAE-cellulose column was subjected to a 25% ammonium sulfate precipitation, no significant pellet formed after centrifugation, therefore this step was eliminated from the procedure.

The resuspended pellet from the 45% ammonium sulfate precipitation was subjected to size exclusion chromatography on a 2.5 x 110 cm Sephadex® G-150 column (Figure II.5). Active fractions from the Sephadex® G-150 column were combined and brought to 1 M ammonium sulfate concentration for further purification by hydrophobic interaction chromatography (HIC). Several different HIC supports were investigated and the greatest degree of purification with the highest recovery of L-PADH activity was obtained using a butyl Sepharose® resin (Figure II.6).

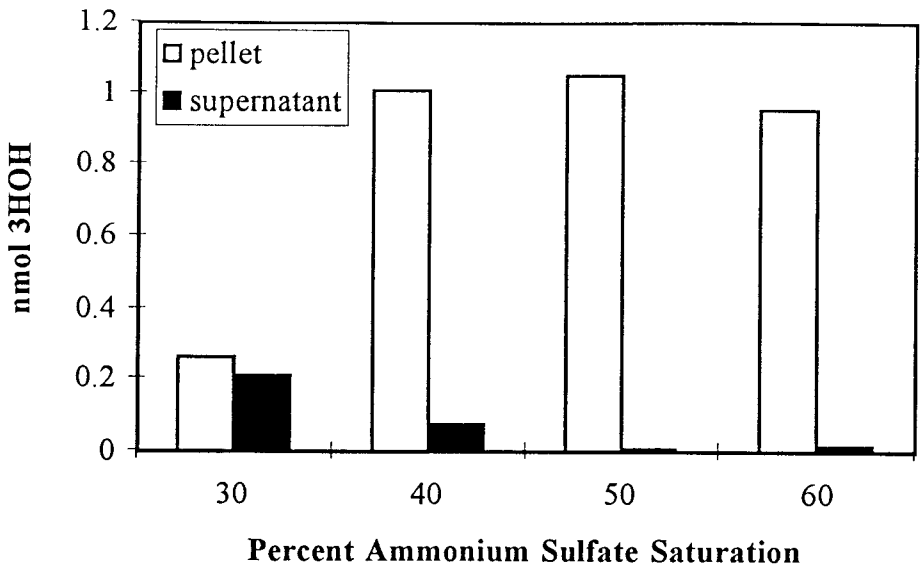

Figure II.4 Ammonium sulfate precipitation of L-PADH activity. The open columns represent the amount of activity found in the pellet at the corresponding percent ammonium sulfate. The filled columns represent the activity in the supernatants.

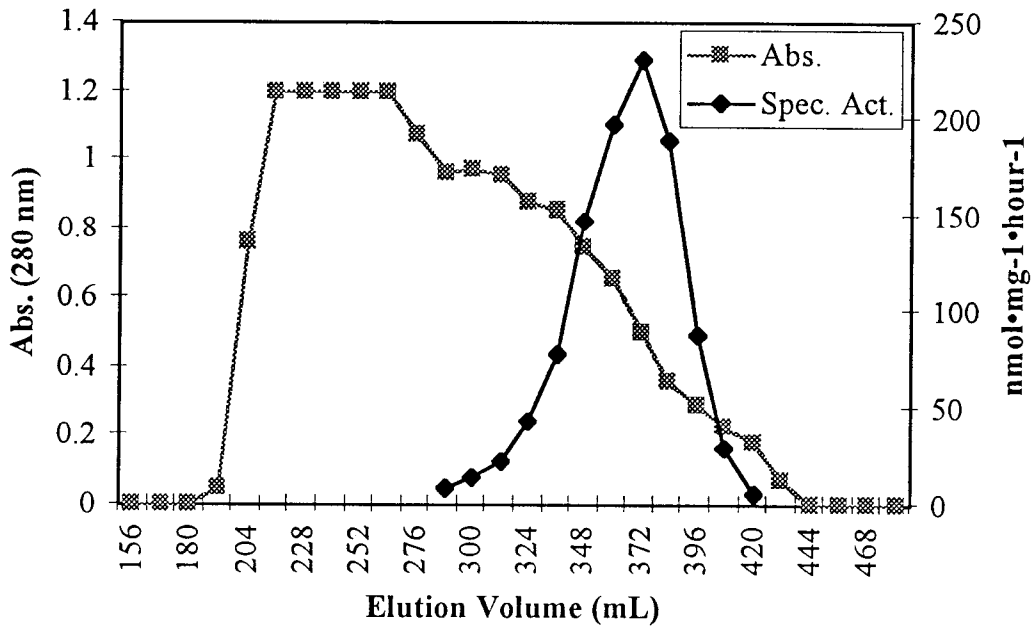

Figure II.5 Profile of elution volume versus absorbance at 280 nm for Sephadex® G-150 size exclusion column. The specific activity of L-PADH is superimposed.

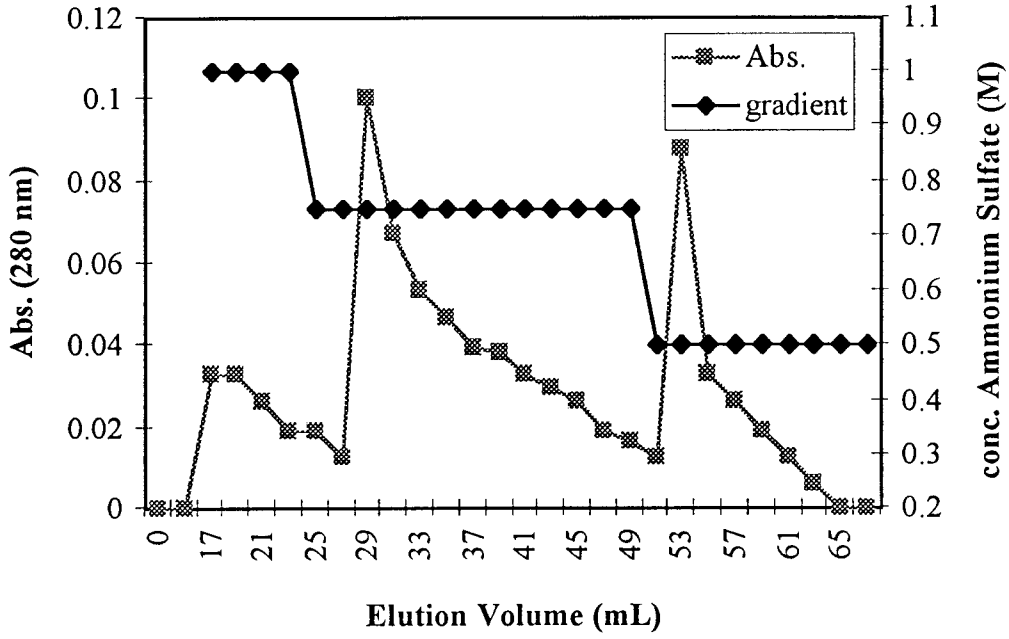

Figure II.6 Purification of L-PADH on butyl Sepharose® column. The UV absorbance is superimposed on the ammonium sulfate gradient. The active enzyme eluted in the 0.5 M ammonium sulfate fraction.

Fractions from the HIC column containing L-PADH activity were pooled and concentrated using an Amicon Centriprep 10 centrifugal concentrator. The retentate was transferred to a dialysis cartridge (10 kDa molecular weight cutoff) and dialyzed versus low salt buffer.

The final purification step involved anion exchange chromatography on a DEAE Fast Flow column. A linear gradient from 10 mM KCl to 200 mM KCl was applied over 50 minutes. Because L-PADH eluted from a previous DEAE column at approximately 100 mM KCl, fractions near 100 mM KCl on the DEAE Fast Flow column were initially assayed for L-PADH activity. The resulting chromatogram is shown in Figure II.7.

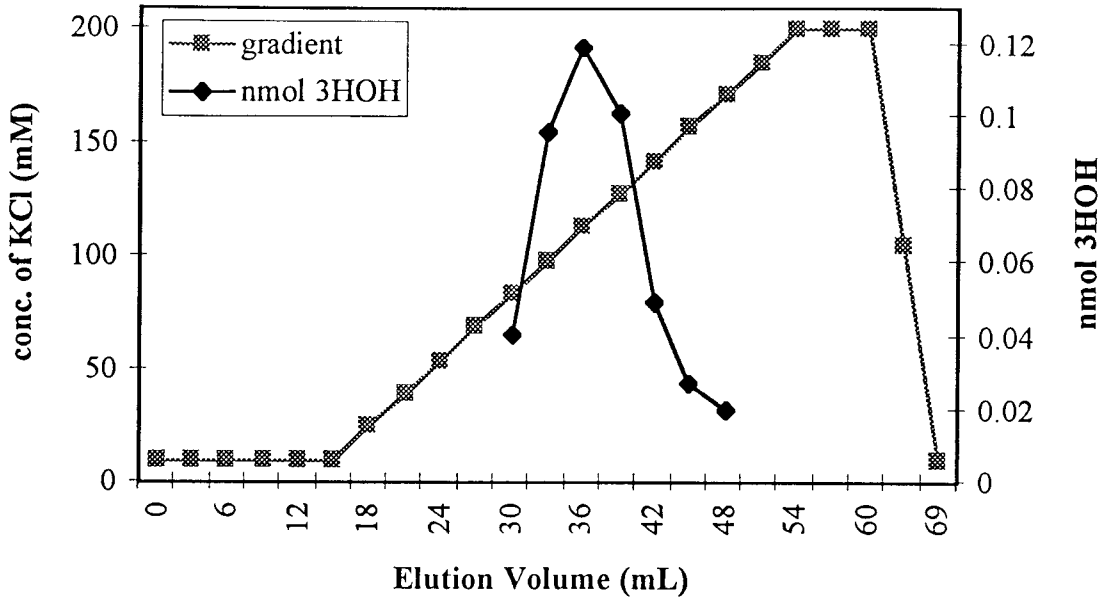

Figure II.7 Elution profile of L-PADH activity from a DEAE Fast Flow column. The activity is superimposed over the linear gradient from 10 mM KCl to 200 mM KCl.

The active fractions from the DEAE Fast Flow column were pooled and concentrated. This procedure resulted in a 300 fold purification of L-PADH with a final specific activity of approximately 400 nmol•mg^{-1}•hr^{-1}. A summary of the L-PADH purification is shown in Table II.2.

Table II.2 Partial purification of L-pipecolic acid dehydrogenase from 100 g of rabbit kidney cortexes.

Fraction	Protein (mg)	Total Activity (nmol ^{3}HOH•hr^{-1})	Specific Activity (nmol ^{3}HOH•mg^{-1}•hr^{-1})	Purif. (fold)	% Rec.
cell free	5440	7400	1.4	------	-------
DEAE	996	7400	7.6	5.6	100
AS ppt	227	3341	14.7	10.8	45.1
G150	20.5	2688	131	96.4	36.3
Butyl	2.2	547	249	183	7.4
Dialysate	1.7	349	206	151	4.7
DEAE FF	0.3	119	396	291	1.6

Fractions from the individual steps in the partial purification of L-PADH were analyzed by SDS-PAGE (Figure II.8). Protein bands at approximately 65, 41, 26 and 15 kDa continued to appear upon further attempts at purification. From the gel shown in Figure II.6 the most likely L-PADH candidate appears to be one of the bands at approximately 41 kDa which were enriched through the purification scheme. However, with the data on hand the other proteins at 15, 26, 65 kDa and the higher molecular weight bands cannot be discounted.

Other chromatographic techniques: Several other chromatographic techniques were investigated for use in the purification of the rabbit dehydrogenase. Most of these techniques provided little or no increase in specific activity of the enzyme.

CM-cellulose cation exchange chromatography was studied on a small scale at several pH values for the ability to bind L-PADH. CM-cellulose was slurried in 0.5 mL of buffer at various pH values between 6.5 and 8.5. Cell free extract (0.2 mL) was added to the slurry and gently rocked at 4 °C. Cell free extract without CM-cellulose was also rocked at 4 °C and served as a control. The slurry was centrifuged and the buffer decanted and assayed for L-PADH activity (Table II.3).

Table II.3 The effect of pH on binding of L-PADH to CM-cellulose resin.

10 mM Buffer (pH)	Activity (CPMs) in supernatant
control (pH = 7.5)	549
PIPES (pH = 6.5)	322
HEPES (pH = 7.0)	274
HEPES (pH = 7.5)	457
Tris (pH = 8.0)	575
Tris (pH = 8.5)	748

It appeared that much of the activity was found in the supernatant at all pH values. The difference in apparent activities is probably due to the pH of the buffers; L-PADH is most active at pH 8.5. However these experiments were performed on a very small scale and therefore a larger scale experiment was tried. A 5 mL CM-cellulose column was equilibrated in 50 mM BisTris, 10 mM KCl, pH 6.8. When a sample containing L-PADH was chromatographed on the column the activity was found only in the unretained fractions with no increase in specific activity.

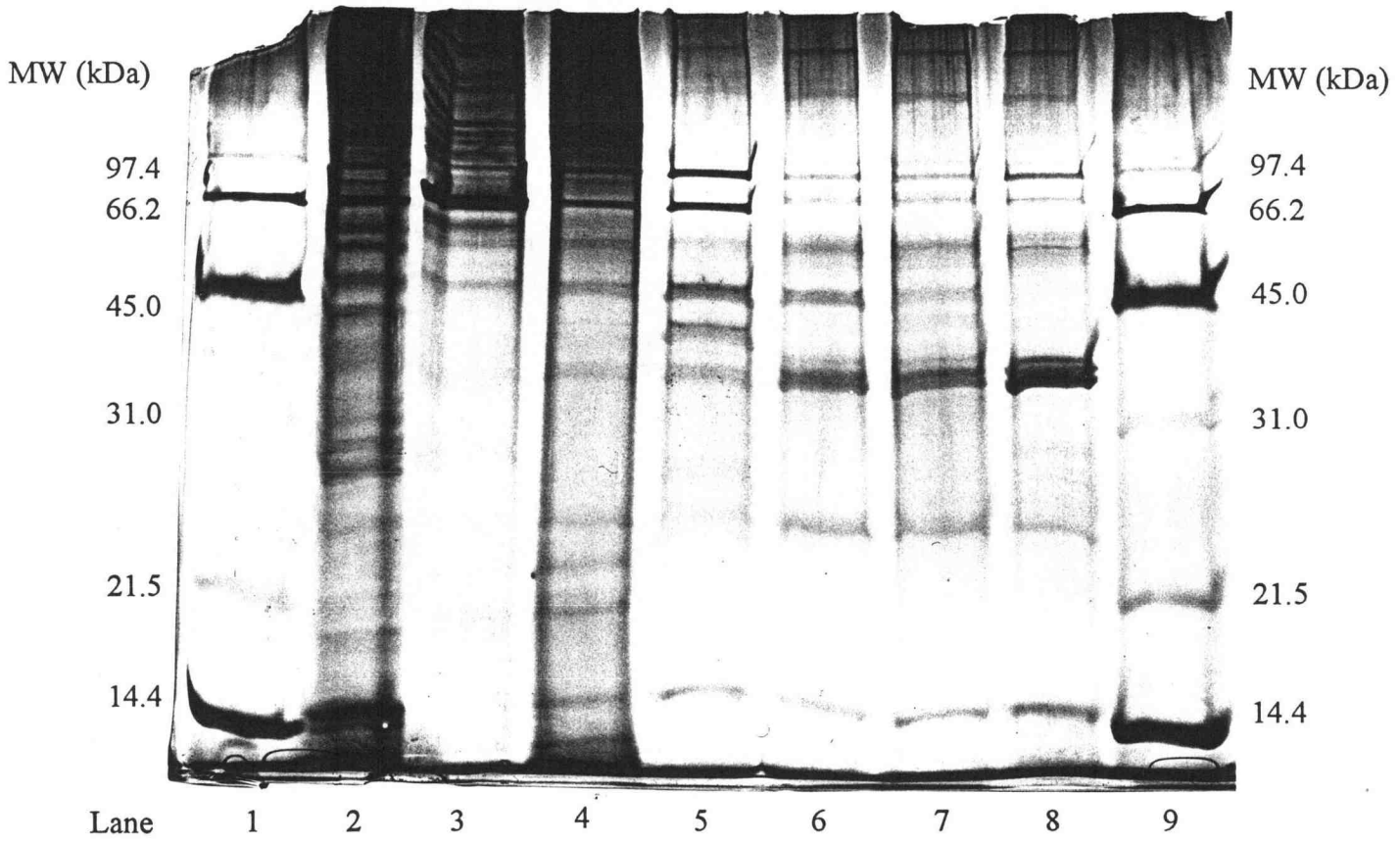

Figure II.7 Silver stained 12.5% SDS-polyacrylamide gel of the L-PADH purification. Lane 1) molecular weight standards, 2) cell free extract, 3) DEAE-cellulose, 4) 45% ammonium sulfate precipitate, 5) Sephadex G-150, 6) butyl Sepharose, 7) dialysate, 8) DEAE fast flow, 9) molecular weight standards.

Hydrophobic interaction chromatography using a phenyl Sepharose® column was used in the purification of the primate oxidase, therefore this method was investigated for purification of the rabbit dehydrogenase. Initially the column appeared to provide some purification of the enzyme when loaded in a buffer containing 25% ammonium sulfate and then eluted in 20% propylene glycol. However, these results were not reproducible. Further attempts to purify L-PADH with a phenyl column demonstrated that the enzyme bound, but would not elute even when the column was washed with 50% propylene glycol followed by 1 M KCl buffer.

Several other hydrophobic interaction chromatography medias were investigated including butyl, octyl, ether, and methoxy resins. The methoxy and octyl columns were not successful in binding the enzyme or increasing the specific activity of L-PADH. The dehydrogenase did bind to the ether column, but little activity was recovered. The resin to which the hydrophobic functional groups were attached appeared to make a difference in the binding of the enzyme. Several supports including, Sepharose® and agarose from Pharmacia, Toyo-pearl® from TosoHaas, and Macro-Prep® a ceramic support from BioRad were tried. In all of the HIC studies, the protein was loaded in 1 M ammonium sulfate, 50 mM HEPES, pH 7.4, and gradients were run with decreasing concentrations of salt. If no activity was found after reaching 0 M ammonium sulfate, dilute solutions of propylene glycol or high concentrations of KCl were used to elute any remaining protein off the column. The butyl Sepharose® resin gave the best recovery of activity (20%) with the highest specific activity (250 $nmol \cdot mg^{-1} \cdot hr^{-1}$).

Immobilized metal affinity chromatography was investigated using an imidodiacetic acid resin. The resin was charged with either copper, nickel, or zinc. The protein was loaded in low KCl buffers and eluted with increasing concentrations of imidazole. L-PADH bound to the column regardless of which metal ion was used. Copper was selected as the immobilized metal in these studies because recovery of L-PADH activity was greatest using copper and L-PADH eluted at lower concentrations of imidazole than when zinc or nickel were used. Very low activity was found in the imidazole fractions eluted from the copper column. It was later determined that imidazole, at concentrations as low as 25 mM, inhibited the activity of the dehydrogenase. Dialysis to remove the imidazole did not lead to increased recovery of activity. The enzyme activity was not recovered when high salt buffers were used to elute the protein. No L-PADH activity was detected in the 0.1 M EDTA solution used to remove the metal ions from the resin.

Three gel filtration chromatography resins were examined; Sephadex® G-150, G-100, and G-75. The column dimensions for each were 2.5 x 110 cm and the columns were

equilibrated in 250 mM KCl, 50 mM potassium phosphate, pH 7.4. The highest specific activity recovered was associated with the Sephadex® G-150 column. An increase of approximately nine fold in purification was achieved with this step.

Because L-pipecolic acid dehydrogenase appears to utilize a non-covalent flavin in the oxidation of L-PA, purification on a FAD agarose affinity column was attempted. L-PADH was loaded onto a 0.8 mL column in 10 mM KCl, 50 mM HEPES, pH 7.4. Two elution buffers were used, one contained 1 M KCl and the other contained 5 mM FAD. Under both conditions L-PADH activity was only seen in the unretained material. Neither column resulted in an increase in the purity of the enzyme.

Attempts were also made to purify the enzyme using strong anion and cation exchange resins. These included types Mono S and Mono Q from BioRad. The Mono S is a strong cation exchange column that contains an alkyl sulfonate functional group. The Mono Q is a strong anion exchange column that utilizes a quaternary amine. Both columns were equilibrated and loaded in low salt buffers and were run on low pressure and high pressure chromatography systems. The L-PADH activity in each case was found in the unretained portion, and no other significant UV absorbing peaks appeared even after washing with 1 M KCl buffer.

Purification of L-PADH on a Macro-Prep® hydroxylapatite column was also tried. Hydroxylapatite can be used to separate acidic, basic, and neutral proteins. L-PADH was loaded according to manufacturers directions onto a 1 mL column in 0.1 M potassium phosphate, pH 5.8, and washed with the same buffer. A step gradient of 0.2, 0.3, and 0.4 M potassium phosphate, pH 5.8, followed. The activity for the dehydrogenase and the only UV absorbance detected was in the unretained fractions and no increase of specific activity was found as a result of this purification step.

Dye affinity chromatography was attempted to purify the rabbit dehydrogenase further and possibly isolate the enzyme involved in the oxidation of α-ASA to α-AAA. The second enzyme involved in the degradation of L-PA catalyzes the oxidation of α-ASA to α-AAA and has been shown to be NAD^+ dependent.[45] Affi-Gel Blue-Gel® dye affinity resin from BioRad was used with linear and step gradients of increasing KCl concentrations. The dual column ion exchange assay was used to analyze the column fractions for activity. No significant amounts of ^3HOH or α-[^{3}H]-AAA were detected.

In addition to various soft gel techniques, HPLC methods were also employed to purify L-PADH. Two POROS® resins from PerSeptive Biosystems were tried using a Beckman BioSys 510 chromatography system. A cell free extract that had been subjected to ammonium sulfate precipitation was applied to a weak anion exchange column (POROS® PI) equilibrated in 10 mM KCl, 50 mM HEPES, pH 7.4. A linear gradient

from 10 mM to 1 M KCl in 50 mM HEPES, pH 7.4, was used to elute bound protein. No increase in purification was obtained when the specific activity of the active POROS® fractions were compared to that from the DEAE-cellulose step in the standard protocol. Active L-PADH material from a Sephadex® G-150 column was applied to the weak anion exchange column and run under the same conditions. No significant increase in purification was observed. Chromatography on a phenyl (POROS® HP2) column was also performed. After the protein was loaded in 1 M ammonium sulfate, 50 mM HEPES, pH 7.4, a linear gradient from 1 M to 0 M ammonium sulfate applied. Very little activity was recovered and there was no increase in purification.

Mitochondria isolation: A mitochondria isolation was attempted in order to reduce total protein levels in the crude extracts. Frozen rabbit kidney cortexes were homogenized and centrifuged according to the procedure described in Material and Methods. Only very low glutamate dehydrogenase activity was detected in the soluble kidney mitochondria fraction when compared to the standard. No activity was observed in the mitochondrial pellets. Commercially available rabbit kidney cortexes are dipped in liquid nitrogen and shipped in dry ice for preservation. These results suggest the thawed tissue contained mitochondria that had already lysed. Effective isolation of the mitochondria would therefore not be possible without fresh tissue.

Native molecular weight estimation. Two calibrated size exclusion columns (Sephadex® G-100 and G-75) were used to estimate the native molecular weight of L-PADH. Protein standards of known molecular weight were applied to the columns and the V_e was measured for each. A standard curve was produced by plotting the log of the molecular weight versus the V_e/V_o ratio. L-PADH was then chromatographed on both columns and the V_e was measured at the point where the specific activity was highest (Figure II.9). The native molecular weight of L-PADH was estimated from the standard curve. The highest specific activity of L-PADH eluted at a $V_e/V_o = 1.42$ on the G-100 column, providing a molecular weight estimate of 45 kDa. The calculated L-PADH V_e/V_o from the calibrated G-75 column was 1.24, corresponding to a molecular weight of 52 kDa. L-PADH native molecular weight was estimated at approximately 49 kDa.

Native gel electrophoresis. Native gel electrophoresis was explored in order to identify which of the protein band(s) identified using SDS-PAGE might be associated with L-PADH activity. If a substantial amount of activity could be recovered from native gel electrophoresis then this procedure could be attempted on a preparative scale. Native gel electrophoresis was first tried using slab gels in order to conserve materials and enzyme as well as to determine whether activity could be recovered. The manual for

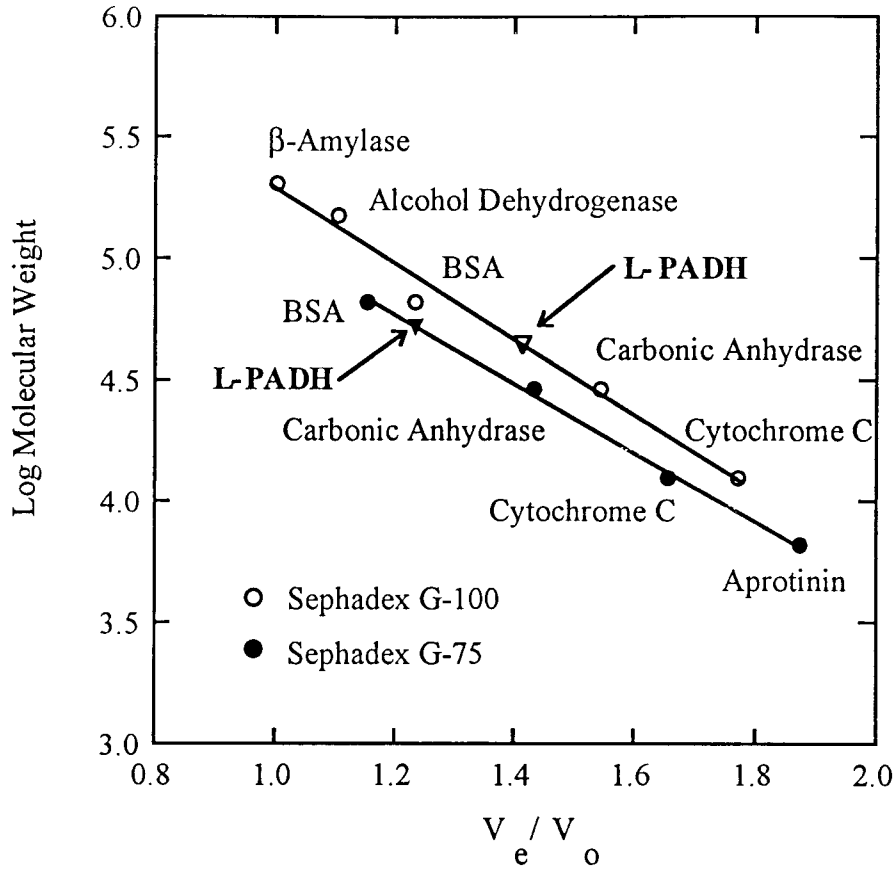

Figure II.9 Native molecular weight determination of L-PADH by calibrated gel filtration chromatography.

preparative native gel electrophoresis suggested that the first attempt at native gel electrophoresis follow the Ornstein-Davis system.[55,56,67] This discontinuous system consisted of a stacking gel and sample loading buffer at pH 6.8, and resolving gel and tank buffer at pH 8.8 (Table II.4).

The gels were divided into 1 cm slices and each slice analyzed for L-PADH activity using the radioassay. The first conditions tried were a 10 % resolving gel with a 4% stacking gel electrophoresed for 14 hours. Low amounts of activity were recovered from the initial native gel, therefore several experiments were conducted in order to optimize the electrophoretic conditions. Some of these conditions included altering the percent acrylamide in the resolving gel, or eliminating the stacking gel. A 6% gel was utilized to obtain further migration of the protein, however the enzyme mobility was unchanged for electrophoresis times up to 12 hours. In almost every case a diffuse band

of protein was seen at the top of the native gel. These results suggested that a different buffer system should be tried.

Table II. 4 Conditions of native gel electrophoresis using the Ornstein-Davis buffer system.

Gel composition	run time (hr)	R_f of activity
4% stacker, 10% gel	14	0.4
4% stacker, 6 % gel	12	0.4
6% gel only	12	0.4
10% gel only	19	0.4

The Jovin system, a discontinuous system, consists of cathode buffer at pH 7.25, anode buffer at pH 5.9, and both gel and sample buffers at pH 6.61.[57] The protein migration increased using this buffer system and longer electrophoresis times (Table II.5).

Table II.5 Conditions and results using the Jovin native gel system.

Gel composition	run time (hr)	R_f of activity	% recovery
4% stacker, 10% gel	14	0.2	19.7
4% stacker, 6 % gel	8	0.2	20.8
4% stacker, 6 % gel	24	0.7	15.0

SDS-PAGE analysis of the slices containing activity from the 6% native gel run for 24 hours are shown in Figure II.8. SDS-PAGE displayed an enriched band at 26 kDa and bands near 50 kDa, but the bands at 41 kDa and 15 kDa on the SDS-polyacrylamide gel from the purification procedure were not seen. These results suggested that L-PADH may be a monomer of approximately 50 kDa, or a homodimer consisting of 26 kDa monomers.

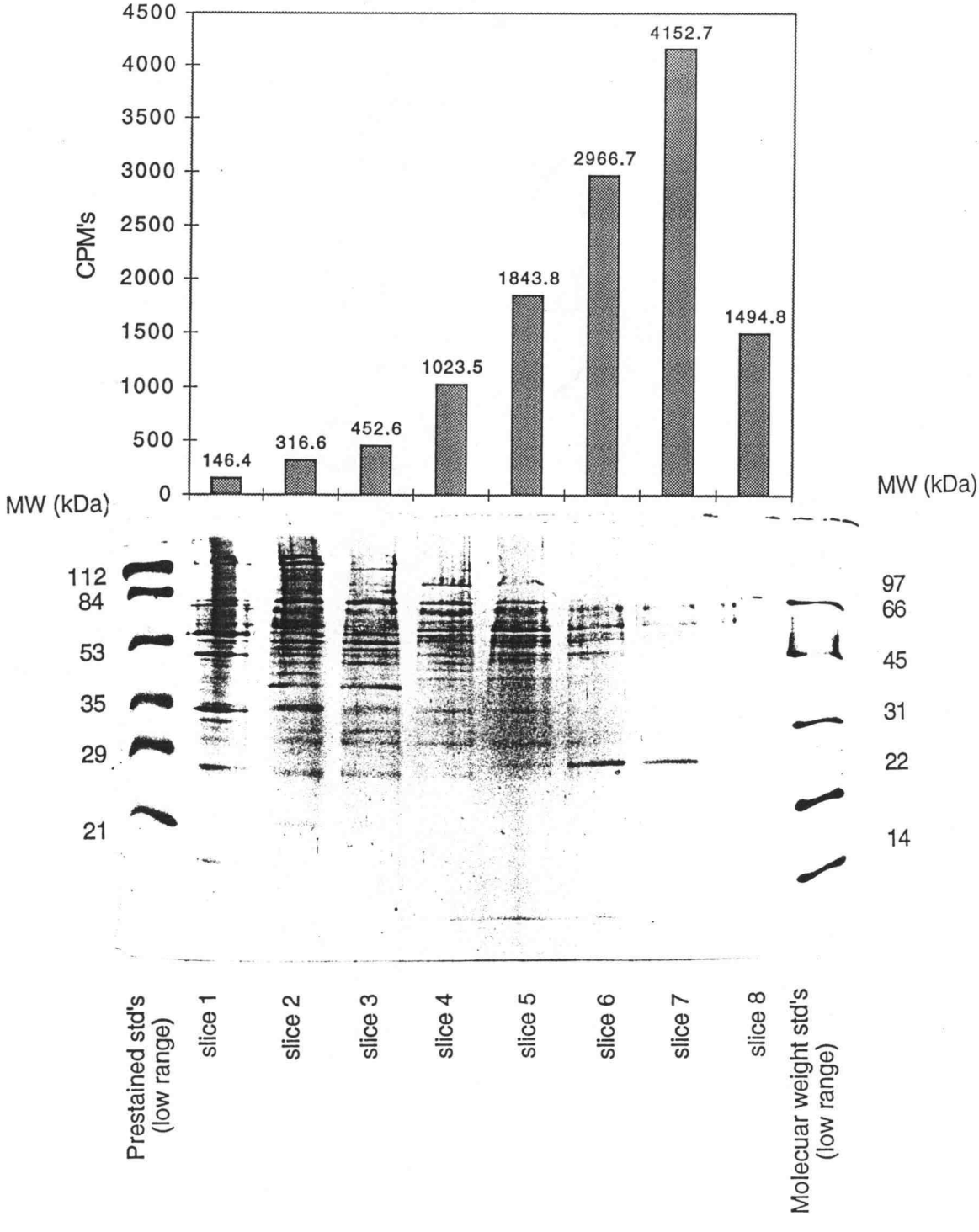

Figure II.10 L-PADH activity and corresponding SDS-polyacrylamide gel of gel slices from a 6% native gel run in the Jovin buffer system.

Preparative native gel electrophoresis was carried out using a BioRad model 491 Prep Cell®. Initial studies with the Jovin buffer system resulted in no recovery of activity and an apparent focusing of the protein near the top of the gel. Because the protein appeared to focus on the preparative gel, native electrophoresis on slab gels were reinvestigated using a different buffer system. The McLellan system is a continuous buffer system in which the gel buffer and tank buffer are the same.[58] Of the three native gel systems tried, the McLellan system gave the highest percent recovery with the furthest migration of L-PADH activity (Table II.6).

Table II.6 Conditions and results using the McLellan native gel system.

Gel composition	run time (hr)	R_f of activity	% recovery
4% stacker, 6% gel	12	0.3	35.0
4% stacker, 6% gel	20	0.8	19.2
6% gel, no stacker	12	0.6	23.5
4% stacker, 10% gel	24	0.6	18.6

Preparative native gel electrophoresis was attempted again using the McLellan buffer system and a 6% acrylamide native resolving gel (5 cm) with a 4% stacking gel (1 cm). Twenty milligrams of protein from an active HIC fraction was applied to the gel. Electrophoresis was carried out at 10 watts for 7 hours and L-PADH was detected by the radioassay (Figure II.11). Two peaks were detected by UV absorbance (280 nm). The first peak was due to the sample loading dye and the second peak contained protein. L-PADH activity was detected between the two UV peaks, however there was no increase in the specific activity. This lack of increase in specific activity was likely due to the denaturing of active protein during electrophoresis. SDS-PAGE analysis of these protein fractions revealed the presence of the usual four protein bands (*ca.* 65, 41, 26, and 15 kDa).

Western blot analysis. Further attempts to identify L-PADH on a SDS-polyacrylamide gel utilized Western blot analysis. Polyclonal rabbit antibodies were generated towards the purified monkey L-PO and provided as a gift from Prof. Stephanie J. Mihalik (Johns Hopkins University).[47] Partially purified rabbit dehydrogenase samples were electrophoresed on a 12.5% SDS-polyacrylamide gel and electroblotted onto a nitrocellulose membrane. The membrane was incubated with the rabbit anti-

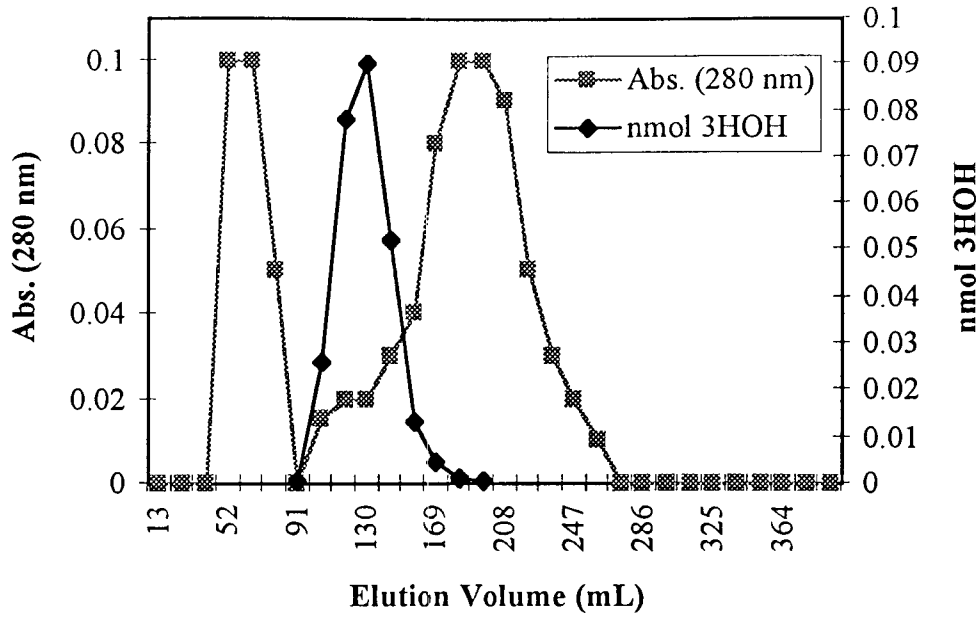

Figure II.11 Elution profile of L-PADH activity from a preparative electrophoresis experiment. The first UV active peak is the sample loading buffer with dye. The second UV absorbing peak is protein eluted from the native gel. L-PADH activity was detected shortly after the loading dye eluted.

monkey antisera and goat anti-rabbit IgG conjugated with alkaline phosphatase. No protein bands were visualized upon development as described in Material and Methods. The L-PADH samples did not cross-react with the rabbit anti-monkey antisera. Active L-PADH samples from a 6% native gel were also subjected to SDS-PAGE and Western blot analysis, but the rabbit anti-monkey antisera did not cross-react with these L-PADH samples either.

Immunoprecipitation. The Western blot analysis of L-PADH may not have been successful because of the small amount of protein applied to the gels. Therefore, an immunoprecipitation protocol was conducted on a larger protein sample. The rabbit anti-monkey antisera (1:170) was incubated with partially purified L-PADH samples and purified L-PO as a control. Protein A Sepharose® was added and the mixtures were centrifuged. The supernatants were assayed for activity using the radioassay. No loss of activity was observed in the L-PADH samples, but the L-PO control resulted in an 80% decrease of activity. Both the supernatants and the pellets were analyzed by SDS-PAGE. Only the rabbit anti-monkey antisera band at 50 kDa was observed in lanes

containing the pellet fractions. There were no disappearance of bands in the L-PADH supernatants, but the L-PO supernatant fraction did not display the 46 kDa band of the purified L-PO. It was possible that the L-PO 46 kDa band was hidden under the large rabbit anti-monkey antisera band at 50 kDa in the pellet fraction. Thus, L-PADH does not cross-react with the rabbit anti-monkey antisera.

Native gel activity stain. This is a modification of an experiment originally used to identify the protein band on a native gel that contained sarcosine dehydrogenase.[60] Sarcosine dehydrogenase possesses a covalent flavin that is reduced during the oxidation of sarcosine.[68] Phenazine methosulfate a substitute electron acceptor, reoxidizes the covalent flavin on the enzyme. Phenazine methosulfate is reoxidized by *p*-nitro blue tetrazolium chloride which, when reduced, precipitates forming a blue band in the gel. Sections of a 6% native gel containing L-PADH activity were incubated in the assay mixture (0.1 M potassium phosphate, pH 7.4, 0.1 M L-PA, 0.04 mM FAD, 0.2 mM PES, and 0.5 mM NBT) overnight. *p*-Nitro blue tetrazolium chloride did not precipitate anywhere in the gel.

Isoelectric point. In order to determine the pI of L-PADH in a non-homogeneous sample, preparative isoelectric focusing experiments were performed using a BioRad Rotofor Cell®. Several different sets of conditions were attempted using broad range ampholytes (pH 3-10), (Table II.7).

Table II.7 Conditions and results of preparative isoelectrofocusing of L-PADH.

Cell (mL)	wattage	run time (hr)	active fraction	pH	comments
20	12	5	none	---	-----
60	15	6	fraction 7	5.7	precipitation
20	12	2	fraction 6	5.5	precipitation
20	12	2	none	---	5% glycerol
20	10	3	none	---	15% glycerol

L-PADH activity was only detected in fractions that contained protein that precipitated during focusing. The pH of these fractions were pH 5.5 and 5.7. An approximation of the pI of L-PADH was estimated to be 5.6 from these experiments. Glycerol was added to the protein sample in order to maintain the solubility of the

protein. Glycerol prevented precipitation, but no activity was detected in any fraction. Inactive fractions that had been solubilized with glycerol were concentrated and resuspended in pH 8.5 buffer. The buffer exchanged fractions were assayed for activity, but none was recovered. SDS-PAGE analysis of these inactive fractions revealed that protein was present in fractions 6, 7, 8 and 9, corresponding to pH values of approximately 5.0 to 6.5. These experiments suggest that the pI of L-PADH is approximately 5.6.

Kinetic parameters. A dye-linked assay using DCPIP was used to determine the kinetic parameters of L-PADH with L-PA as substrate.[61] During the oxidation of L-PA, two electrons are transferred to FAD. FAD is reoxidized by PES which is then reoxidized by DCPIP. Oxidized DCPIP is dark blue in color and when reduced becomes colorless. The progress of the reaction can be followed by a decrease in absorbance at 600 nm (Scheme II.3).

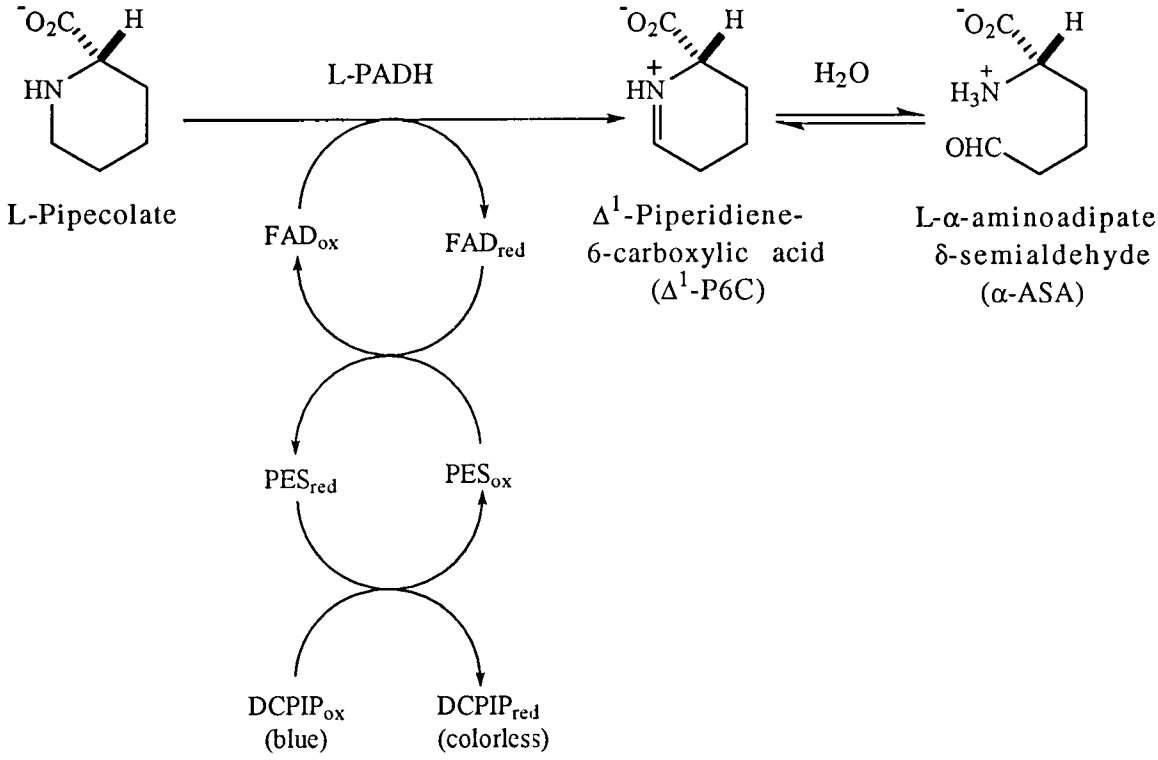

Scheme II.3

Using the DCPIP spectrophotometric assay, the oxidation of L-PA by L-PADH was shown to follow Michaelis-Menten kinetics (Figure II.12). The assay mixtures were kept at 37 °C and contained 12 mM Tris, pH 8.5, 5 mM KCl, 0.1 mM DCPIP, 1 mM KCN, 0.07 mM FAD, 0.7 mM PES, and 25 µL of partially purified L-PADH in a total volume of 0.5 mL. The reactions were initiated with L-PA at concentrations ranging from 0.1 mM to 5 mM . The K_m^{app} of L-PADH was estimated to be 0.88 mM with a V_{max} of 0.02 µmol•mg^{-1}•min^{-1}.

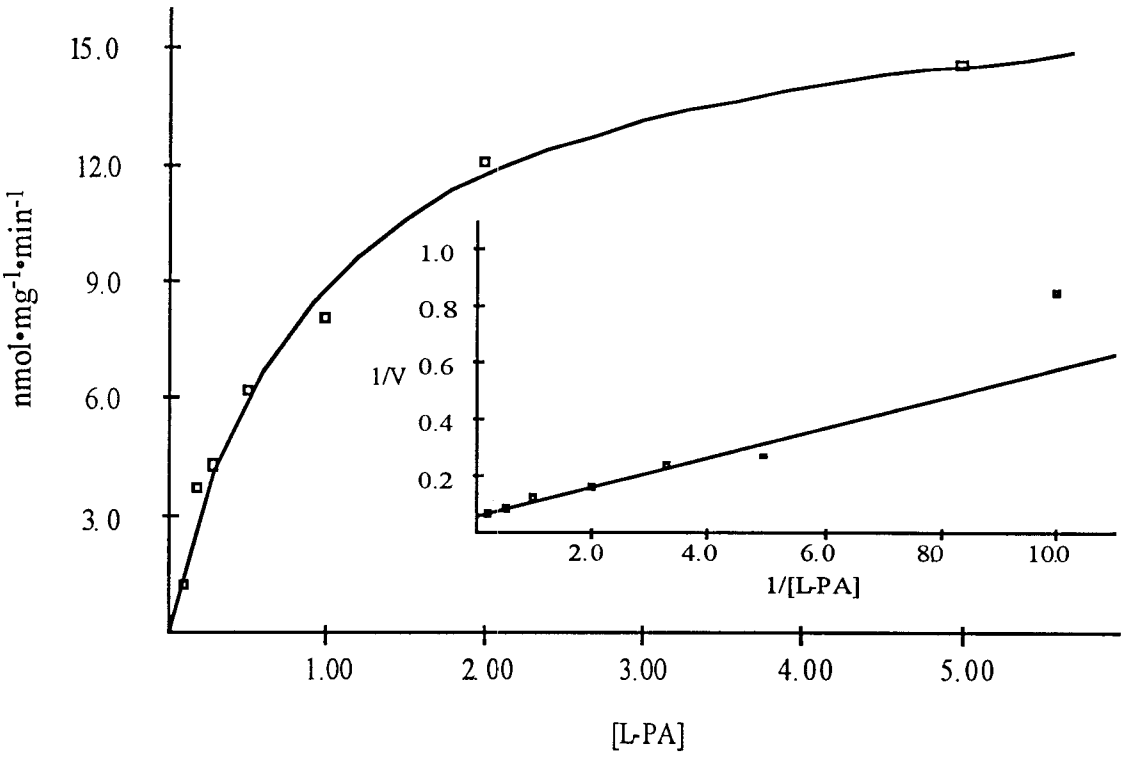

Figure II.12 Non-linear regression analysis of the kinetic study of L-PADH. L-PA concentrations ranged from 0.1 mM to 5 mM. *Inset*: Lineweaver-Burke plot of the results.

Stereochemical course of oxidation of L-PA by L-PADH. The stereochemical course of the oxidation of L-PA by L-PADH was investigated using L-PA stereospecifically deuterated at C-6.[62] L-[6*R*-^{2}H]-PA and L-[6*S*-^{2}H]-PA were incubated with L-PADH at 1 mM final concentrations and the rate of oxidation was measured using

the DCPIP assay. Unlabeled L-PA was used as a control. The initial reaction rates were obtained from the linear portion of the progress curves (Figure II.13).

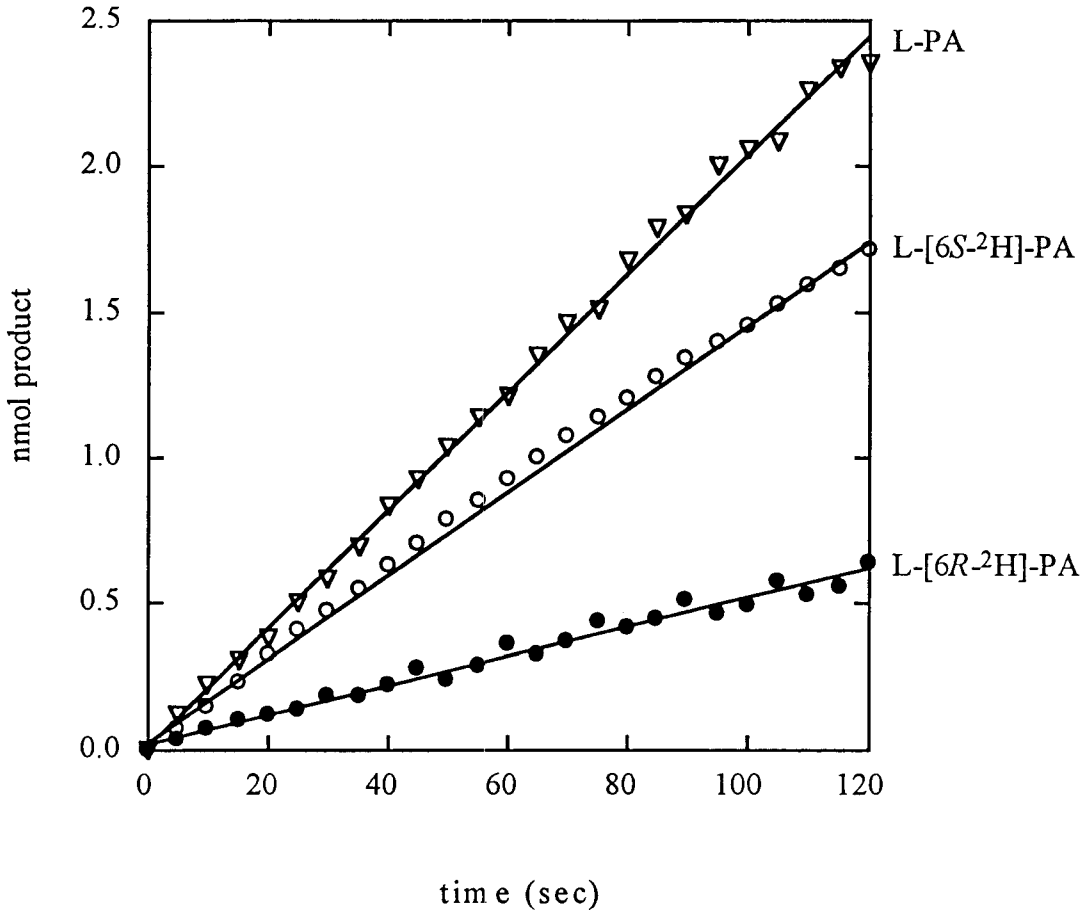

Figure II.13 Time course for the oxidation of L-[6*R*-^{2}H]-PA and L-[6*S*-^{2}H]-PA by L-PADH.

A rate of 0.020 nmol product•mg^{-1}•sec^{-1} was determined for L-PA. The observed rates for L-[6*R*-^{2}H]-PA and L-[6*S*-^{2}H]-PA were 0.005 and 0.014 nmol product•mg^{-1}•sec^{-1}, respectively. These data suggest that a primary isotope effect is observed with L-[6*R*-^{2}H]-PA as the substrate with a k_H/k_D of 4.1. Turnover of L-[6*S*-^{2}H]-PA displayed a significantly lower isotope effect, k_H/k_D=1.4. These data suggest that the *pro*-6*R* hydrogen of L-PA is abstracted by L-PADH during the oxidation process and that the hydrogen abstraction is at least partially rate limiting.

Turnover product. The isolation of the turnover product of L-PADH was important for many reasons, primarily to compare L-PADH with L-PO. The first chemically stable product of L-PA degradation has been shown to be α-AAA in both the monkey and the rabbit.[45] The immediate product of the enzymatic oxidation of L-PA in the rabbit has not been identified, but α-ASA has been shown to be the turnover product of monkey L-PO.[66] The isolation of the L-PADH turnover product would also facilitate the investigation of the mechanism of oxidation by L-PADH using alternate substrates, thus providing useful comparative information between L-PO and L-PADH. Phenylisothiocyanate and 9-fluorenylmethyl chloroformate were used in order to derivatize the turnover product of L-PADH. These derivatives offer high sensitivity and allow the separation of various amino acids by HPLC. Other procedures were tried in order to determine the turnover product of L-PADH. These included formation of a bisulfite adduct, NaB^3H_4 treatment and α-AAA detection. The following describes the results from these experiments.

Phenylisothiocyanate (PITC): PITC reacts with amino acids and produces derivatives that can be separated by HPLC. L-PADH was incubated overnight with an excess of L-PA. The turnover product of L-PO has been characterized as α-ASA and therefore L-PO was also incubated overnight under these conditions and used as a control to establish the retention time of the derivatized α-ASA.[66] The assay mixtures were derivatized with PITC and analyzed by reverse phase (C_{18}) HPLC. The L-PO sample produced two peaks: a peak that contained the PITC derivative of L-PA and a peak with a shorter retention time. Because α-ASA is expected to be more polar than L-PA, it was believed that this peak was the PITC derivative of α-ASA. This was confirmed when L-PO was incubated with L-[$^3H_5$]-PA and both peaks from HPLC analysis contained radioactivity. L-PADH samples produced only the peak that contained the PITC derivative of L-PA. When L-PADH was incubated with L-[$^3H_5$]-PA, treated with PITC, and analyzed by HPLC, the only radioactivity detected was in the L-PA peak. It was concluded that PITC did not react with the turnover product of L-PADH.

9-Fluorenylmethyl chloroformate (FMOC): FMOC reacts with secondary amino acids to form stable, fluorescent derivatives. L-PADH was incubated with FAD, PES, and an excess of L-PA for 0, 0.5, 1, 2, 4, and 8 hours. FMOC was added to the enzyme mixtures and the solutions were extracted with ether. The aqueous layer was concentrated to dryness and the solid was dissolved and analyzed by HPLC using a reverse phase (C_{18}) column. Several peaks appeared from HPLC analysis. None of the peaks areas increased with time and no new peaks were evident even after 8 hours. It was concluded that FMOC did not derivatize the L-PADH turnover product.

Reduction with tritiated sodium borohydride: To investigate the possibility of trapping Δ^1-P6C and showing that it is an intermediate in the oxidation of L-PA by L-PADH, NaB^3H_4 was used to reduce Δ^1-P6C back to L-PA containing a tritium label.[65] A diagram for the reduction of Δ^1-P6C with sodium boro[^{3}H]hydride is shown in Scheme II.4.

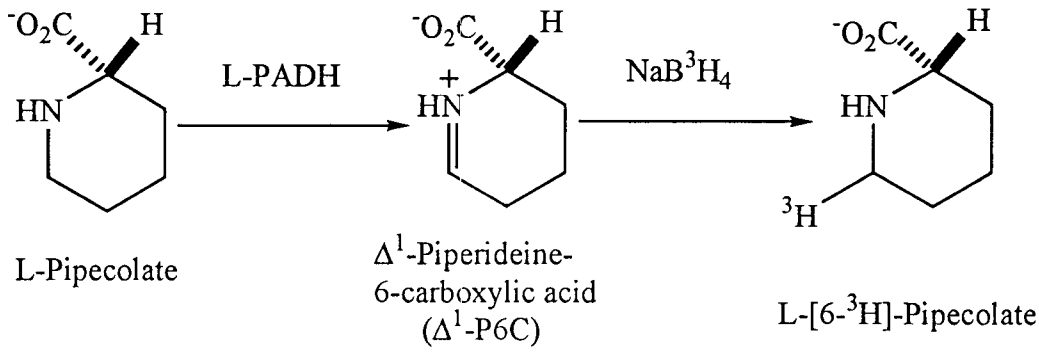

L-Pipecolate

Δ^1-Piperideine-6-carboxylic acid (Δ^1-P6C)

L-[6-^{3}H]-Pipecolate

Scheme II.4

L-PADH was incubated with excess L-PA and then NaB^3H_4 was added to the mixture. The reaction was quenched with HCl and the mixture was applied to a Dowex 50 column. L-PA was eluted from the column using 1 M NH_4OH and concentrated to dryness. The solid was resuspended and subjected to TLC analysis in 7:3 EtOH:NH_4OH. Nitrogen compounds were detected with ninhydrin. The TLC plates were cut into sections and the silica gel was scraped off and assayed for radioactivity. Although a ninhydrin positive spot appeared with the same R_f of L-PA (0.88), no radioactivity was associated with it.

Formation of α-ASA/Bisulfite adduct: This procedure was developed as an assay for L-PO activity in the human liver.[66] Sodium bisulfite reacts with aldehydes to produce a bisulfite adduct. With L-PO, sodium bisulfite reacts with α-ASA to form a bisulfite adduct with a net negative charge and allows separation form L-PA (Scheme II.5). In the standard enzyme radioassay α-ASA binds to the Dowex 50W-X8 cation exchange resin. The bisulfite adduct of α-ASA is negatively charged and will not be retained by the Dowex 50W-X8 column. The bisulfite adduct will therefore pass through the cation exchange resin.

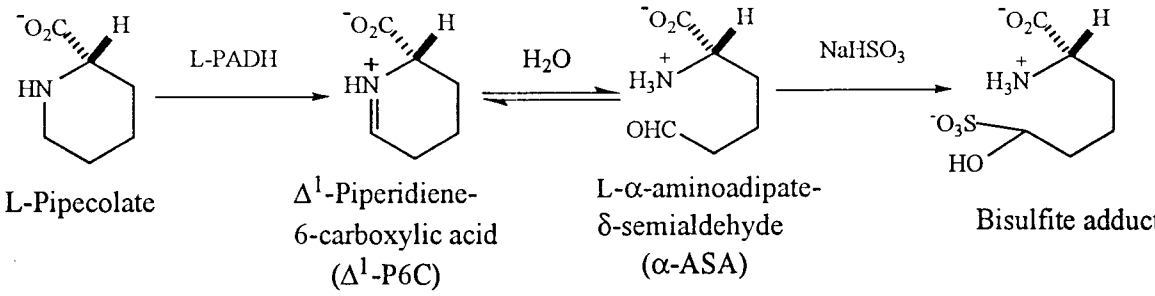

Scheme II.5.

L-PADH was incubated with FAD, PES, L-[$^3H_5$]-PA and sodium bisulfite. The enzyme mixture was applied to a 2 mL Dowex 50W-X8 cation exchange column and the column was washed with 4.5 mL of ddH_2O. The water fraction was evaporated to dryness and resuspended, but no radioactivity was detected in the resuspended solid. The resuspended solid was analyzed by TLC in 7:3 EtOH:NH_4OH. The resuspended solid did not contain a ninhydrin positive spot. These results suggest that α-ASA is not a released product of L-PADH

α-Aminoadipic acid detection: Crude rabbit kidney cortex homogenate was incubated at 37 °C for one hour with FAD, PES, L-[$^3H_5$]-PA, and NAD^+. The NAD^+ cofactor is required for α-ASA dehydrogenase, which converts α-ASA to α-AAA. The enzyme mixtures were applied to a dual column system consisting of AG 1X anion exchange and Dowex 50W-X8 cation exchange resins. The columns were washed with ddH_2O, and the AG 1X anion exchange and Dowex 50W-X8 cation exchange resins were stripped with HOAc and NH_4OH, respectively. The ddH_2O wash and the HOAc and NH_4OH fractions were concentrated to dryness and dissolved in ddH_2O. These fractions were analyzed by paper chromatography on Whatman #1 filter paper in 7:3 EtOH:H_2O. A smeared ninhydrin positive spot appeared for both the AG 1X and Dowex 50W-X8 fractions. The paper was cut into sections and assayed for radioactivity. The sections that had the greatest activity were used to measure the R_f values. The R_f values from monkey preparations were determined previously and reported as 0.91 for L-PA and 0.61 for α-AAA.[45] The R_f values of the rabbit sample from the Dowex 50W-X8 column (L-PA) was 0.9 and that from the AG-1X column (α-AAA) was 0.7. This confirms that the rabbit kidney extracts produce α-AAA, however an intermediate between L-PA and α-AAA has not been identified and isolated.

DISCUSSION

L-Pipecolic acid dehydrogenase has been partially purified 300 fold from rabbit kidney cortex. L-PADH has a molecular weight of approximately 50 kDa and may be a monomer or a homodimer consisting of 26 kDa subunits. This protein has an estimated pI of 5.6 and a pH optimum of 8.5. The K_m of L-PADH for L-PA is 0.88 mM with an observed V_{max} of 0.02 $\mu mol \cdot min^{-1} \cdot mg^{-1}$.

The purification procedure utilized herein has identified some of the properties of L-PADH. The enzyme appears to be an acidic protein with an estimated pI of 5.6. The ability of L-PADH to bind a DEAE resin at pH 7.4 coupled with the inability to bind to a CM resin at pH 6.5 further suggests that L-PADH is an acidic protein.

Although L-PADH is a soluble enzyme, it exhibits some hydrophobic character based on its interaction with HIC resins. L-PADH binds irreversibly to a phenyl-substituted resin, but can be eluted from a butyl-substituted resin which is weaker in hydrophobicity.

Other techniques that provided an increase in the purification of L-PADH with substantial recovery of activity were ammonium sulfate precipitation and size exclusion chromatography. L-PADH precipitated with ammonium sulfate over a broad range of 25 to 45% saturation, and resulted in a two fold increase in specific activity. Size exclusion chromatography provided the greatest increase in purification, nine fold, of any single step. Of the three size exclusion resins tried, the Sephadex® G-150 gave the greatest increase in purification of L-PADH.

Native gel electrophoresis which separates proteins by mass and charge, two characteristics that together would appear to make a protein unique, did not facilitate the purification of L-PADH. Multiple protein bands were present in the SDS-PAGE analyses of native gel fractions containing L-PADH activity.

Western blot analysis of L-PADH with rabbit anti-monkey antisera was investigated as a means to identify the L-PADH band on a SDS-polyacrylamide gel. The rabbit anti-monkey antisera did not cross-react with any protein in active L-PADH fractions or native gel sections. Immunoprecipitation experiments using the rabbit anti-monkey antisera did not result in a loss of soluble L-PADH activity.

Several experiments were carried out in order to elucidate the turnover product of L-PADH. It has been suggested that the oxidation of L-PA produces Δ^1-P6C which is in equilibrium with its open chain form α-ASA.[23] Both PITC and FMOC react with amino acids and these compounds were used to derivatize Δ^1-P6C and/or α-ASA. No derivatization of Δ^1-P6C or α-ASA was observed in L-PADH samples when PITC and

FMOC were used. Another means by which Δ^1-P6C can be detected as the turnover product of L-PADH utilized tritiated sodium borohydride to reduce Δ^1-P6C back to L-PA containing a tritium label. No detection of radioactivity was observed in the recovered L-PA. Sodium bisulfite was added in order to produce a bisulfite adduct of α-ASA, however no reaction was detected. When crude rabbit kidney homogenates were incubated with FAD and NAD^+, α-AAA was detected. This suggests that the final product in the oxidation of L-PA in rabbit preparations is α-AAA. The inability to isolate or detect the intermediate between L-PA and α-AAA suggests that the turnover product of L-PADH is either not released or is produced in amounts below the level of detection.

It is important to compare mitochondrial L-PADH with other amino acid dehydrogenases, specifically proline dehydrogenase. Proline dehydrogenase isolated from *Escherichia coli* and *Salmonella typhimurium* are both multifunctional enzymes that catalyze the oxidation of L-proline to L-glutamate via Δ^1-pyrroline-5-carboxylate.[69,70] In the rat L-proline dehydrogenase only catalyzes the oxidation of L-proline to Δ^1-pyrroline-5-carboxylate.[71] From our data it is difficult to conclude whether or not L-PADH is a multifunctional enzyme, although the only turnover product that has been identified is α-AAA. However, L-PADH has a native molecular weight of only 50 kDa and the multifunctional proline dehydrogenases mentioned above have native molecular weights of 260 kDA. Although proline dehydrogenase has been shown to oxidize L-PA analogs, L-proline did not significantly inhibit the activity of L-PADH suggesting that the L-PADH activity is specific for L-PA.[45,70]

A comparison of the enzymes involved in mammalian pipecolate oxidation reveals several fascinating differences and similarities; particularly properties such as subcellular location, mode of cofactor association and reoxidation, and kinetic parameters. A comparison of the primate oxidase and rabbit dehydrogenase is summarized in Table II.8. Rabbit mitochondrial L-PADH is a soluble enzyme of approximately 50 kDa, while L-PO is a monomer at 46 kDa and is a membrane-associated protein located in the peroxisomes of primates.[47] L-PO has a covalently bound flavin cofactor and molecular oxygen serves as the electron acceptor in the catalyzed oxidation of L-PA, the formation of H_2O_2 being the result.[47] L-PADH also utilizes a flavin cofactor, but it requires the addition of an electron acceptor such as phenazine ethosulfate in order to reoxidize the flavin back to the catalytically active form. It has been suggested that L-PADH eventually shuttles the electrons from L-PA through the electron transport chain.[45]

Table II.8 Comparison of L-pipecolic acid oxidase and L-pipecolic acid dehydrogenase.

Characteristic	L-PO	L-PADH
species	primates	lower mammals
location	peroxisomes	mitochondria
soluble vs. insoluble	membrane associated	soluble
cofactors	covalently bound FAD	activity stimulated by addition of FAD
	H_2O_2 is produced	requires addition of an electron acceptor
K_m (L-PA)	3.7 mM	0.88 mM
Vmax (L-PA)	2.1 μmol•min^{-1}•mg^{-1}	0.02 μmol•min^{-1}•mg^{-1}
6-H abstraction	*pro 6R*	*pro 6R*
Molecular Weight	46 kDa	~50 kDa
pH Optimum	8.5	8.5
pI	8.9	estimated at 5.6

The K_m of L-PO for L-PA is four fold higher than that of L-PADH, suggesting that L-PO has a lower affinity for L-PA as a substrate. The maximum velocity of L-PO is 100 fold greater than the dehydrogenase, but it should be noted that the value determined for the dehydrogenase is from a non-homogenous enzyme. Both enzymes have a pH optimum of 8.5 and abstract the *pro-6R* hydrogen from L-PA.[72] While the pI of the oxidase is 8.9 indicating that it is a basic protein, the pI of the dehydrogenase is estimated to have an acidic isoelectric point at pH 5.6.

When the yeast oxidase and bacterial dehydrogenase are also considered (*cf.* Chapter I), the evolutionary relationship of the enzymes involved in L-PA oxidation is quite intriguing. Both the rabbit dehydrogenase and the dehydrogenase from *P. putida* require FAD, however the rabbit enzyme is soluble while the bacterial enzyme is membrane bound.[32] The oxidase from primates is membrane-associated and possesses a covalent FAD, but the yeast oxidase from *R. glutinis* has been reported as requiring no cofactor.[40,41] Ultimately, sequence information at the DNA level will be required to establish the convergent or divergent evolution of the enzymes involved in pipecolic acid oxidation.

CHAPTER III

ALTERNATE SUBSTRATES OF L-PIPECOLIC ACID DEHYDROGENASE

INTRODUCTION

Early studies by Mihalik and Rhead revealed that primate and rabbit tissue preparations containing L-pipecolic acid (L-PA) oxidizing activity were highly specific for L-PA as substrate.[45] In order to verify that L-PA was not being oxidized by enzymes in other pathways with structurally related substrates, it was shown that glutamate, L-proline and D-alanine had little effect on cell-free studies of L-pipecolate oxidation, thus excluding significant contributions to the observed activity by saccharopine dehydrogenase, proline dehydrogenase or D-amino acid oxidase.

The purification of Rhesus liver L-PO allowed more extensive studies on the oxidation of alternate substrates to be conducted.[47,73] Purified L-PO demonstrated high specificity for L-PA when compared with activity towards numerous D- and L-amino acids.[73] The only compounds other than L-PA that served as substrates for L-PO were L-proline and sarcosine, which were oxidized at rates 23% and 10%, respectively, of that seen for L-PA.[47,73]

In the initial studies describing the subcellular location of rabbit L-PADH in the kidney mitochondria, several structural analogs were evaluated for the ability to affect L-PA oxidation. Piperidine, L-proline, nipecotic acid (piperidine-3-carboxylic acid) and cis-2,4-piperidine dicarboxylic acid were shown to have a negligible effect on the reaction.[45] Identification of alternate substrates may provide useful information for comparative studies of L-PO and L-PADH. Furthermore, analogs of L-PA could also serve as valuable probes to study the exact chemical mechanisms catatalyzed by these enzymes.

A number of L-PA analogs have been synthesized and tested as potential inhibitors of, and alternate substrates for, L-PO and L-PADH. Many of these compounds were designed as inhibitors of the primate oxidase to serve as potential leads to therapeutic agents for treating convulsive disorders and as pharmacological tools to study the role of L-PA in the mammalian CNS. The design of these compounds was based on a proposed mechanism for flavin-dependent oxidation of L-PA (Scheme III.1).

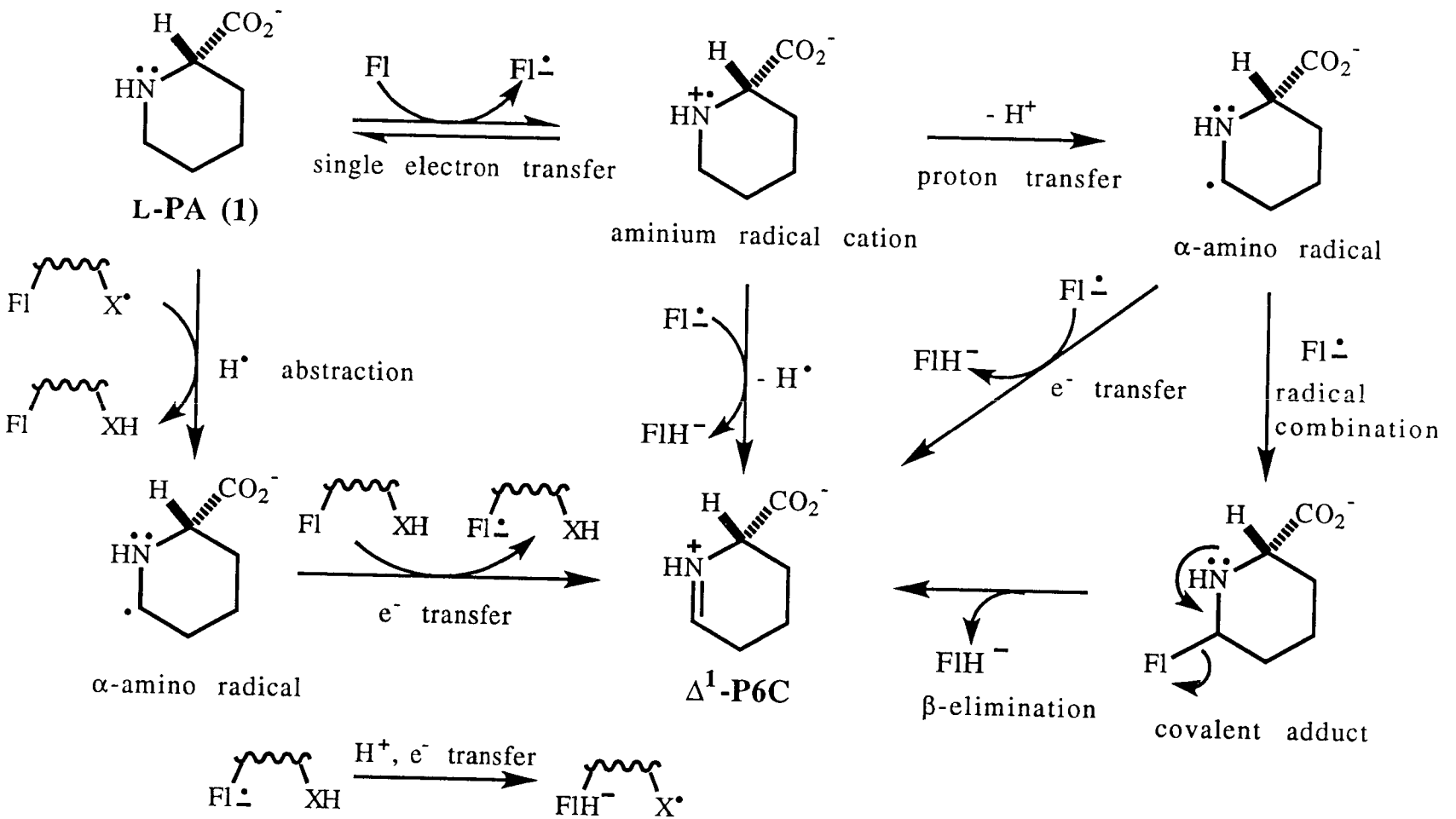
L-PA (1)
single electron transfer
aminium radical cation
- H+
proton transfer
α-amino radical
H• abstraction
- H•
e- transfer
radical combination
α-amino radical
e- transfer
Δ1-P6C
FlH−
β-elimination
covalent adduct
H+, e- transfer

Scheme III.1

This scheme was developed from mechanistic data proposed for other highly-studied flavin-dependent amine oxidases such as monoamine oxidase.[74,75] Compounds were sought which could stabilize or relocate a possible α-amino radical generated during the oxidation process. Alternate substrates which can stabilize a radical intermediate may function as better substrates and as valuable tools for spectroscopic studies of these enzymes. Stabilization of a highly reactive radical species may also lead to alternate decomposition pathways resulting in enzyme inactivation. A delocalized radical may result in a reactive species that combines with an active site radical or abstracts a hydrogen from the enzyme leading to inactivation.

MATERIALS AND METHODS

Materials. All biochemicals and solvents were purchased from Sigma, Fisher and VWR. All buffers and solutions were made using double deionized and filtered (0.45 mm) water (NANOpure, Barnstead). L-PA (**1**), L-proline (**2**), sarcosine (**5**), 3,4-dehydro-L-proline (**6**), and (*R*)-thiazolidine-4-carboxylic acid (**11**) were purchased from Sigma. Compound **7** (4,5-dehydro-L-pipecolic acid) was prepared by Dr. Mark Zabriskie. The nitrogen substituted analogs, *N*-nitroso-L-pipecolate (**3**) and *N*-methyl-L-pipecolate (**4**), were synthesized by Hua Qi. (*R,S*)-1,3-Oxazane-4-carboxylic acid (**8**), (*S*)-hexahydropyrimidine-4-carboxylic acid (**9**), (*R,S*)-piperazine-2-carboxylic acid (**10**), (*S*)-1,3-thiazane-4-carboxylic acid (**12**), (2*R*, 4*S*)-2-methyl-1,3-thiazane-4-carboxylic acid (**13a**), (2*S*, 4*S*)-2-methyl-1,3-thiazane-4-carboxylic acid (**13b**), (3*S*)-1,4-thiazane-3-carboxylic acid (**14**), (3*S*)-1-oxo-1,4-thiazane-3-carboxylic acid (**15a**), and (3*S*)-1,1-dioxo-1,4-thiazane-3-carboxylic acid (**15b**) were gifts from Xi Liang. Spectrophotometric studies were carried out on a Hitachi U2000 spectrophotometer.

Kinetic studies of L-PADH with L-pipecolic acid analogs. Several L-PA analogs were synthesized as potential inhibitors of L-PO.[76,77] These compounds were evaluated for activity as substrates and/or inhibitors of L-PADH using the DCPIP spectrophotometric assay described in Chapter II.[61] The reaction mixture contained 12 mM Tris, pH 8.5, 5 mM KCl, 0.1 mM DCPIP (ε = 21.5 L•mmol-1•cm-1), 1 mM KCN, 0.07 mM FAD and 0.7 mM PES. A sample of L-PADH (62 μg), partially purified to the point of a Sephadex® G-150 size exclusion column, was used in the assays. Controls omitting enzyme or substrate analogs were conducted for all compounds. A substantial decrease in absorbance was often seen in the controls without L-PADH and this value

was subtracted from the rate of the complete reaction mixture. The Enzyme Kinetics software package from Trinity Software was used to analyze the data.

Time-dependent inactivation. The reaction mixture contained 12 mM Tris, pH 8.5, 5 mM KCl, 0.1 mM FAD, 1.0 mM PES, 5 mM 4,5-dehydro-L-pipecolate (**7**), and 0.45 mg of L-PADH purified to the point of an HIC column in 80 μL total volume. A control without 4,5-dehydro-L-pipecolate (**7**) was also analyzed. The reactions incubated at room temperature. In order to dilute the inhibitor and assay the enzyme for activity, a 10 μL aliquot of the reaction mixture was added to 490 μL of reaction buffer kept at 37 °C containing 12 mM Tris, pH 8.5, 5 mM KCl, 0.07 mM FAD, 0.7 mM PES, 0.1 mM DCPIP, 1 mM KCN, and 5 mM L-PA. The reaction was assayed for activity at 5 minutes, 20 minutes, 1, 4, 8, and 24 hours. The DCPIP reduction was monitored at 595 nm.

RESULTS

Sixteen analogs of L-PA were tested as inhibitors and substrates of partially purified L-PADH. The kinetic data are summarized in Tables III.1, III.2 and III.3. The ability of L-PADH to oxidize L-Proline (**2**) and sarcosine (**5**) was of interest because both proline dehydrogenase and sarcosine dehydrogenase will recognize L-PA as a substrate, albeit a poor one.[78] L-PADH was able to oxidize both of these structural analogs at rates approximately 45% of that observed for L-PA (Table III.1), demonstrating an interesting reciprocal substrate relationship for these three similar flavin-dependent amine oxidases.

The effect of substituents on the pipecolate nitrogen was also tested. *N*-Nitroso-L-PA (**3**) served as a poor substrate for L-PADH with an observed turnover rate 20% of that seen with pipecolic acid at the same concentration. The *N*-methylated analog **4** had no effect on L-PADH activity and also failed to act as a surrogate substrate (Table III.1).

One class of compounds with the potential to increase the stability of a radical intermediate are those with an adjacent double bond, allowing for the formation of a delocalized allylic radical.[79,80] Both 3,4-dehydro-L-proline ($\Delta^{3,4}$-L-proline, **6**) and 4,5-dehydro-L-pipecolate ($\Delta^{4,5}$-L-PA, **7**) served as excellent alternate substrates for L-PADH (Table III.2). Both unsaturated analogs were much more efficiently turned over by L-PADH as demonstrated by the lower K_m and higher V_{max} values compared to L-PA.

Table III.1 L-pipecolic acid homologs and N-substituted L-pipecolic acid analogs tested as substrates/inhibitors of L-PADH.

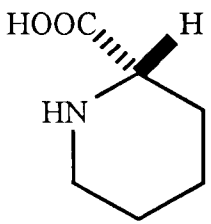

1

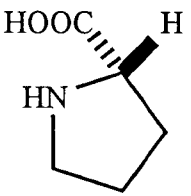

2

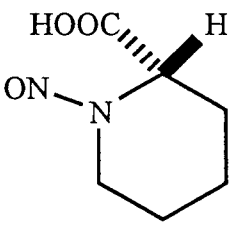

3

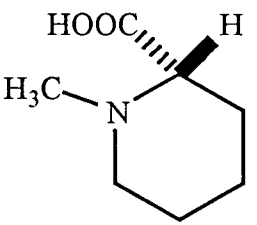

4

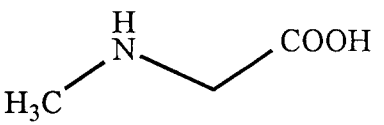

5

Compound	Activity
L-Pipecolic Acid (**1**)	K_m=0.88 mM, V_{max}= 20 nmol•min^{-1}•mg^{-1}
L-Proline (**2**)	At 5 mM: 45% activity relative to L-PA
N-Nitroso-L-Pipecolic Acid (**3**)	At 5 mM: 20% activity relative to L-PA
N-Methyl-L-Pipecolic Acid (**4**)	Not a substrate, no inhibition
Sarcosine (**5**)	At 5 mM: 46% activity relative to L-PA

Table III.2 Dehydro-L-pipecolic acid analogs, oxygen and nitrogen heterocycle analogs of L-pipecolic acid tested as substrates/inhibitors of L-PADH.

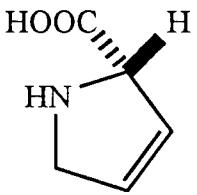

6

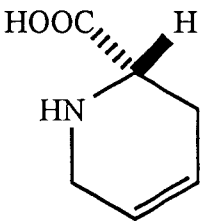

7

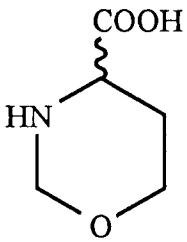

8

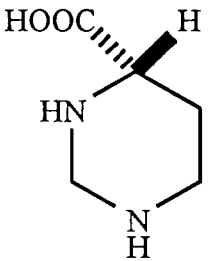

9

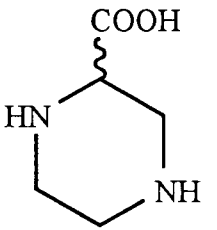

10

Compound	Activity
3,4-Dehydro-L-Proline (**6**)	K_m= 0.71 mM, V_{max}= 180 nmol•mg^{-1}•min^{-1}
4,5-Dehydro-L-Pipecolic Acid (**7**)	K_m= 0.19 mM, V_{max}= 88 nmol•mg^{-1}•min^{-1}
(*R*,S)-1,3-Oxazane-4-Carboxylic Acid (**8**)	Not a substrate, no inhibition
(*S*)-Hexahydropyrimidine-4-Carboxylic Acid (**9**)	At 5 mM: 90% of the activity relative to L-PA
(*R*,S)-Piperazine-2-Carboxylic Acid (**10**)	At 5 mM: 28% of the activity relative to L-PA

Table III.3 Sulfur containing heterocycle analogs of L-pipecolic acid tested as substrates/inhibitors of L-PADH.

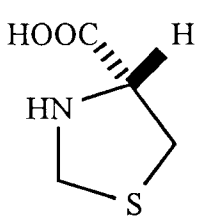

11

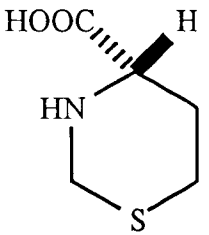

12

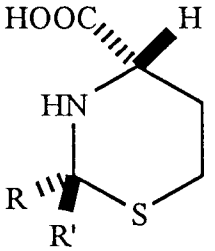

13

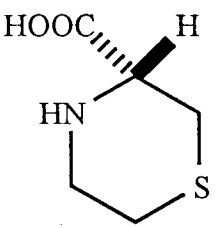

14

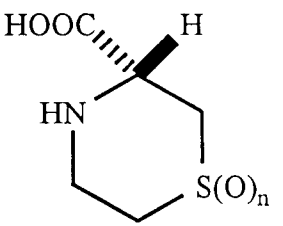

15

Compound	Activity
(*R*)-Thiazolidine-4-Carboxylic Acid (**11**)	K_m= 0.83 mM, V_{max}= 9.4 nmol•min^{-1}•mg^{-1}
(*S*)-1,3-Thiazane-4-Carboxylic Acid (**12**)	K_m= 1.5 mM, V_{max}= 77 nmol•min^{-1}•mg^{-1}
(2*R*, 4*S*)-2-Methyl-1,3-Thiazane-4-Carboxylic Acid (**13a**: R=CH_3, R'=H)	Not a substrate, no inhibition
(2*S*, 4*S*)-2-Methyl-1,3-Thiazane-4-Carboxylic Acid (**13b**: R=H, R'=CH_3)	Not a substrate, no inhibition
(3*S*)-1,4-Thiazane-3-Carboxylic Acid (**14**)	K_m=1.1 mM, V_{max}= 3.1 nmol•min^{-1}•mg^{-1}
(3*S*)-1-Oxo-1,4-Thiazane-3-Carboxylic Acid (**15a:** n=1)	Not a substrate, no inhibition
(3*S*)-1,1-Dioxo-1,4-Thiazane-3-Carboxylic Acid (**15b:** n=2)	Not a substrate, no inhibition

Heteroatoms in the α-position have also been shown to stabilize a carbon-centered radical intermediate.[80] Therefore, the effect of heteroatom substitution in the pipecolate ring was investigated. Substitution of an oxygen atom at position 5 of L-PA produced a compound (**8**) that was not recognized by L-PADH, while nitrogen replacement at position 5 of L-PA yielded a good alternate substrate (**9**) (Table III.2). Moving the nitrogen to the 4 position of L-PA (**10**) results in a three fold decrease in the rate of oxidation when tested at the same concentration.

A series of sulfur containing derivatives of L-PA were also evaluated for their ability to affect L-PADH catalysis. Three thioether derivatives tested (**11**, **12**, and **14**) served as alternate substrates of L-PADH. Compounds **11** (4-thiaproline) and **12** (5-thiapipecolate) have the sulfur in the position α to the site of the radical and proved to be good substrates with kinetic parameters comparable to those for L-PA (Table III.3). Sulfur substitution at position 4, where the sulfur is now β to the radical (**14**), had no effect on V_{max} and large decrease in K_m, thus yielding a modest substrate. Adding a methyl group at position 2 (thiazane numbering) of compound **12** (**13a** and **13b**) eliminates binding to the active site, possibly due to steric effects. Oxidizing the 4-thiapipecolate **14** to the sulfoxide (**15a**) or the sulfone (**15b**) also eliminated the ability of the analog to be oxidized by L-PADH or act as an inhibitor.

Data from kinetics experiments on those L-PA analogs that serve as good substrates for L-PADH are presented in double reciprocal plots (1/V vs. 1/S) in Figure III.1. Of the these compounds, $\Delta^{3,4}$-L-proline (**6**) and $\Delta^{4,5}$-L-PA (**7**) were found to be excellent substrates of the rabbit dehydrogenase with K_ms of 0.71 mM and 0.19 mM, respectively, and were turned over by L-PADH at rates substantially greater than that observed for L-PA. The 4-thiaproline (**11**) exhibits kinetic parameters near those of the natural substrate while the thiapipecolates **12** and **14** were good-to-modest substrates of L-PADH.

DISCUSSION

One of the primary reasons for synthesizing the compounds depicted in Tables III.1, III.2 and III.3 was to develop inhibitors of the primate oxidase which may have use as pharmacological tools or, possibly, provide leads for therapeutic agents to treat convulsive disorders. While rabbit pipecolate dehydrogenase is not a therapeutic target, the availability of these substrate analogs provided the opportunity to probe the active site topology and catalytic differences of the peroxisomal oxidase and mitochondrial

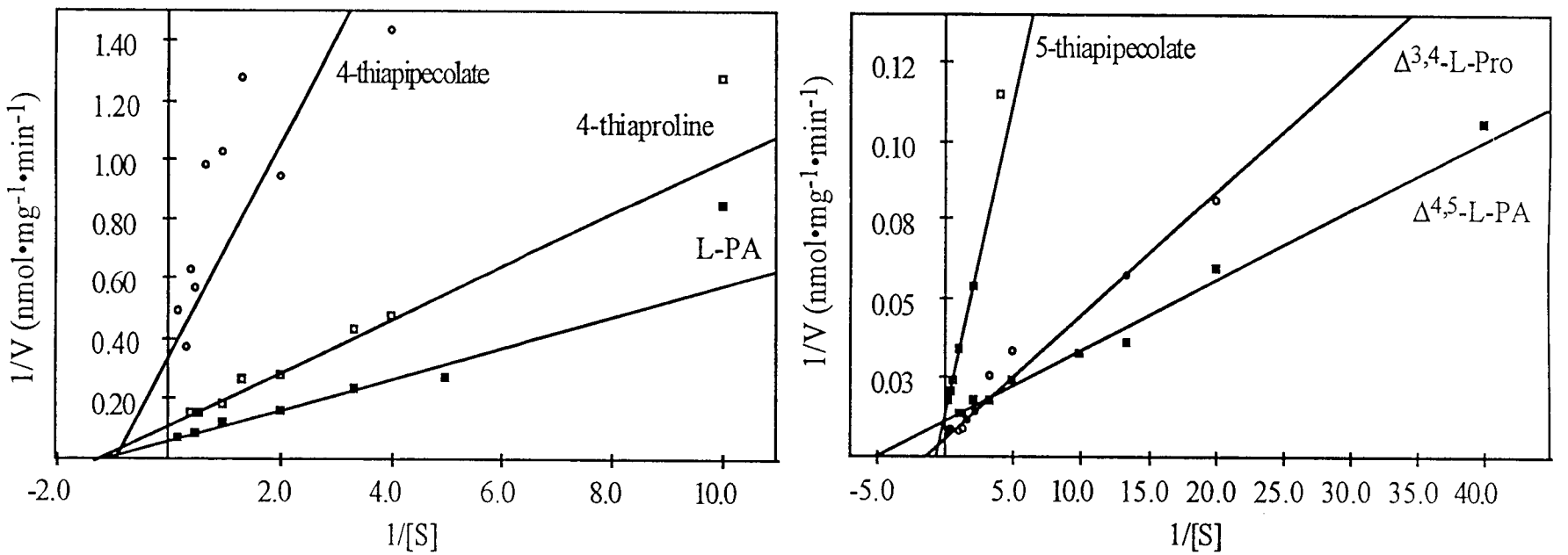

Figure III.1 Double reciprocal plots of L-PADH with L-PA (**1**), $\Delta^{3,4}$-L-Pro (**6**), $\Delta^{4,5}$-L-PA (**7**), 4-thiaproline (**11**), 5-thiapipecolate (**12**), and 4-thiapipecolate (**14**) as substrates.

dehydrogenase. A comparative summary of the interactions of these compounds with Rhesus liver L-PO and rabbit kidney L-PADH is presented in Table III.4.

Table III.4 Comparison of L-pipecolic acid analogs as inhibitors and substrates of L-PO and L-PADH.

Characteristic	L-PO	L-PADH
*K*m (L-PA)	3.7 mM	0.88 mM
*V*max(L-PA)	2.1 μmol•min^{-1}•mg^{-1}	0.02 μmol•min^{-1}•mg^{-1}
Alternate Substrates	L-proline (**2**)	L-proline (**2**)
	sarcosine (**5**)	*N*-nitroso-L-PA (**3**)
	hexahydropyrimidine (**9**)	sarcosine (**5**)
	4-thiapipecolate (**14**)	$\Delta^{3,4}$-L-Pro (**6**)
		$\Delta^{4,5}$-L-PA (**7**)
		hexahydropyrimidine (**9**)
		piperazine (**10**)
		4-thiaproline (**11**)
		5-thiapipecolate (**12**)
		4-thiapipecolate (**14**)
Mechanism-Based Inactivators	4,5-dehydro-L-PA (**7**)	----------
	5-thiapipecolate (**12**)	
Reversible Inhibitors	*N*-nitroso-L-PA (**3**)	
	4-thiaproline (**11**)	
	2*R*-methyl-1,3-thiazane (**13a**)	----------
	2*S*-methyl-1,3-thiazane (**13b**)	
	1-oxo-thiazane (**15a**)	

The comparison of L-PO and L-PADH with pipecolic acid as substrate has been presented in Chapter II and is also included in Table III.4. Other compounds able to function as substrates for both enzymes include the L-PA analogs **2**, **5**, **9**, and **14**.

While the above compounds served as alternate substrates for both L-PO and L-PADH, other L-PA analogs help delineate the differences between the two enzymes. For example, $\Delta^{4,5}$-L-PA (**7**) is a potent time-dependent inactivator of L-PO with a K_I = 0.13 mM and k_{inact} = 2.0 min^{-1}.[81] However, **7** served as an excellent substrate for the rabbit enzyme with K_m = 0.19 mM and V_{max} = 88 nmol•min^{-1}•mg^{-1} and no inactivation was detected even when L-PADH was incubated with 5 mM **7** for 24 hours. The lower homolog of **7**, $\Delta^{3,4}$-L-Pro (**6**), is an excellent substrate of both the dehydrogenase and

oxidase, although at very high concentrations some inhibition of the oxidase was detected. Compound **12**, 5-thiapipecolate, is readily turned over by L-PO, K_m = 0.94 mM and V_{max} = 100 nmol•min^{-1}•mg^{-1} and acts as a poor mechanism-based inactivator K_I = 36 mM and k_{inact} = 0.06 min^{-1}.[76] As is the case with **7**, compound **12** reacts with L-PADH only as a substrate, K_m = 1.5 mM and V_{max} = 77 nmol•min^{-1}•mg^{-1}. The ability of the rabbit dehydrogenase to oxidize these compounds without inhibition is an interesting contrast between L-PO and L-PADH. Further studies on the mechanisms of inhibition of the oxidase, such as determining if the species responsible for inactivation attacks the flavin cofactor or the protein, and sequencing the active sites of both enzymes, may help understand these differences.

Other analogs that highlight differences between the two enzymes include *N*-nitroso-L-PA (**3**), 4-thiaproline (**11**), the sulfoxide **15a**, and the diastereomeric 2-methyl-1,3-thiazanes **13a** and **13b**. *N*-nitroso-L-pipecolic acid (**3**) is the most potent competitive inhibitor yet identified of primate L-PO having a K_i of 0.15 mM.[82] Interestingly, **3** serves as a poor substrate for L-PADH. 4-Thiaproline (**11**) is another potent reversible inhibitor of the monkey oxidase (K_i = 0.30 mM), in surprising contrast to the closely related proline (**2**), $\Delta^{3,4}$-L-Pro (**6**), and 5-thiapipecolate (**12**). However, **11** is readily oxidized by L-PADH (K_m = 0.83 mM, V_{max} = 20 nmol•min^{-1}•mg^{-1}). Compounds **13a** and **13b** are also potent competitive inhibitors of L-PO, both exhibiting inhibition constants of 0.34 mM, yet **13a** and **13b** have no effect on L-PADH activity. Finally, the sulfoxide derivative of 4-thiapipecolate (**15a**) is another competitive inhibitor of L-PO (K_i = 3.1 mM) which has no effect on L-PADH catalysis.

In summary, this study describes differences between L-PO and L-PADH in the ability to interact with sixteen analogs of pipecolic acid. Five pipecolate analogs serve as alternate substrates for both L-PO and L-PADH (Table III.4) and two derivatives (**4** and **8**) do not affect either enzyme, demonstrating a certain degree of similarity in substrate recognition beyond that of L-pipecolic acid. More interestingly, other analogs serve to illustrate marked differences between the two enzymes. For example, six inhibitors of the primate oxidase have been discovered, however no inhibitors of the rabbit dehydrogenase have been detected. Two compounds, *N*-nitroso-L-PA (**3**) and 4-thiaproline (**11**) are turned over by L-PADH and not by L-PO. The discovery of specific inhibitors of L-PADH will be an important step in the continuing characterization of these enzymes.

CHAPTER IV

CONCLUSIONS

L-pipecolic acid is an intermediate of lysine metabolism in various organisms including bacteria, yeast, fungi and mammals. In mammals L-PA catabolism is unusual in that two flavin dependent enzymes have evolved for this process. In primates the enzyme involved in L-PA degradation is a peroxisomal oxidase which has been purified and characterized.[47] In lower mammals L-PA degradation is catalyzed by a soluble, mitochondrial dehydrogenase, but little is known about this enzyme from any source. This thesis details the partial purification and characterization of L-PADH from rabbit kidney cortex and compares physical and catalytic properties of the rabbit dehydrogenase with those of the primate oxidase.

L-PADH has been purified 300 fold from rabbit kidney cortex. The standard purification procedure included homogenization followed by DEAE-cellulose chromatography and 45% ammonium sulfate precipitation. Chromatography on a Sephadex G-150 sized exclusion column preceded hydrophobic interaction chromatography with butyl Sepharose®. After dialysis, DEAE Fast Flow chromatography yielded an enzyme with a final specific activity of 400 $nmol \cdot mg^{-1} \cdot hr^{-1}$.

A comparison of the enzymes involved in mammalian pipecolate oxidation reveals several fascinating differences and similarities; particularly properties such as subcellular location, mode of cofactor association and reoxidation, and kinetic parameters. Rabbit mitochondrial L-PADH is a soluble enzyme of approximately 50 kDa, while L-PO is a monomer at 46 kDa and is a membrane-associated protein located in the peroxisomes of primates.[47] L-PO has a covalently bound flavin cofactor and molecular oxygen serves as the electron acceptor in the catalyzed oxidation of L-PA, the formation of H_2O_2 being the result.[47] L-PADH also utilizes a flavin cofactor, but it requires the addition of an electron acceptor such as phenazine ethosulfate in order to reoxidize the flavin back to the catalytically active form. It has been suggested that L-PADH eventually shuttles the electrons from L-PA through the electron transport chain.[45]

Both enzymes have a pH optimum of 8.5 and abstract the *pro*-6*R* hydrogen from L-PA.[72] While the pI of the oxidase is 8.9 indicating that it is a basic protein, the pI of the dehydrogenase is estimated to have an acidic isoelectric point at pH 5.6. The K_m of L-PO for L-PA is four fold higher than that of L-PADH, suggesting that L-PO has a lower affinity for L-PA as a substrate. The maximum velocity of L-PO is 100 fold greater

than the dehydrogenase, but it should be noted that the value determined for the dehydrogenase is from a non-homogenous enzyme.

Sixteen L-pipecolic acid analogs were investigated for the ability to serve as alternate substrates or inhibitors of the rabbit dehydrogenase and monkey oxidase. Of these, five pipecolate analogs serve as alternate substrates for both L-PO and L-PADH and two derivatives do not affect either enzyme, demonstrating a certain degree of similarity in substrate recognition beyond that of L-pipecolic acid. More interestingly, other analogs serve to illustrate marked differences between the two enzymes. For example, six inhibitors of the primate oxidase have been discovered, yet no inhibitors of the rabbit dehydrogenase have been identified. The discovery of specific inhibitors of L-PADH will be an important step in the continuing characterization of these enzymes.

BIBLIOGRAPHY

(1) Zacharius, P.; Thompson, J. F.; Steward, F. C. *J. Am. Chem. Soc.* **1952**, *74*, 2949-2950.

(2) Zacharius, R. M.; Thompson, J. F.; Steward, F. C. *J. Am. Chem. Soc.* **1954**, *76*, 2908-2912.

(3) Morrison, R. I. *Biochem. J.* **1953**, *53*, 474-478.

(4) Hulme, A. C. *Nature* **1952**, *170*, 659-660.

(5) Harris, G.; Pollock, J. R. A. *J. Inst. Brewing* **1953**, *59*, 28.

(6) Campbell, P. N.; Work, T. S.; Mellanby, E. *Biochemistry* **1951**, *48*, 106-113.

(7) Fowden, L. *Nature* **1951**, *167*, 1030-1031.

(8) Grobbelaar, N.; Steward, F. C. *J. Am. Chem. Soc.* **1953**, *75*, 4341-4343.

(9) Patte, J. C. In *Amino Acids: Biosynthesis and Genetic Regulation*; K. M. Herrmann and R. L. Somerville, Ed.; Addison-Wesley: Reading, MA, 1983; pp 213-228.

(10) Bhattacharjee, J. K. In *Amino Acids: Biosynthesis and Genetic Regulation*; K. M. Herrmann and R. L. Somerville, Ed.; Addison-Wesley: Reading, MA, 1983; pp 229-244.

(11) Rothstein, M.; Miller, L. L. *J. Biol. Chem.* **1954**, *206*, 243-253.

(12) Rothstein, M.; Miller, L. L. *J. Biol. Chem.* **1954**, *211*, 851-858.

(13) Higashino, K.; Tsukada, K.; Lieberman, I. *Biochem. Biophys. Res. Commun.* **1965**, *20*, 285-290.

(14) Grove, J. A.; Young, F.; Roghair, H. G.; Schipke, P. *Arch. Biochem. Biophys.* **1972**, *151*, 464-467.

(15) Hutzler, J.; Dancis, J. *Biochim. Biophys. Acta* **1970**, *206*, 205-214.

(16) Ghadimi, H.; Chou, W. S.; Kesner, L. *Biochem. Med.* **1971**, *5*, 56-66.

(17) Higashino, K.; Fujioka, M.; Yamamura, Y. *Arch. Biochem. Biophys.* **1971**, *142*, 606-614.

(18) Jones, E. E.; Broquist, H. P. *J. Biol. Chem.* **1966**, *241*, 3430-3434.

(19) Saunders, P. P.; Broquist, H. P. *J. Biol. Chem.* **1966**, *241*, 3435-3440.

(20) Grove, J.; Henderson, L. M. *Biochim. Biophys. Acta* **1968**, *165*, 113-120.

(21) Grove, J. A.; Gilbertson, T. J.; Hammerstedt, R. H.; Henderson, L. M. *Biochim. Biophys. Acta* **1969**, *184*, 329-337.

(22) Yagi, K.; Okamura, K.; Takai, A.; Kotaki, A. *J. Biochem. (Tokyo)* **1968**, *63*, 814-815.

(23) Meister, A.; Buckley, S. D. *Biochim. Biophys. Acta* **1957**, *23*, 202-203.

(24) Garweg, G.; von Rehren, D.; Hintze, U. *J. Neurochem.* **1980**, *35*, 616-621.

(25) Hutzler, J.; Dancis, J. *Biochim. Biophys. Acta* **1968**, *158*, 62-69.

(26) Hutzler, J.; Dancis, J. *Biochim. Biophys. Acta* **1975**, *377*, 42-51.

(27) Chang, Y. F. *J. Neurochem.* **1978**, *30*, 347-354.

(28) Chang, Y. F. *Neurochem. Res.* **1982**, *7*, 577-588.

(29) Rao, D. R.; Rodwell, V. W. *J. Biol. Chem.* **1962**, *237*, 2232-2238.

(30) Basso, L. V.; Rao, D. R.; Rodwell, V. W. *J. Biol. Chem.* **1962**, *237*, 2239-2245.

(31) Hartline, R. A.; Rodwell, V. W. *Arch. Biochem. Biophys.* **1971**, *142*, 32-39.

(32) Baginsky, M. L.; Rodwell, V. W. *J. Bacteriol.* **1967**, *94*, 1034-1039.

(33) Calvert, A. F.; Rodwell, V. W. *J. Biol. Chem.* **1966**, *241*, 409-414.

(34) Kase, Y.; Okano, Y.; Kataoka, M.; Miyata, T. *Life Sci.* **1973**, *13*, 867-873.

(35) Giacobini, E.; Nomura, Y.; Schmidt-Glenewinkel, T. *Cell. Mol. Biol.* **1980**, *26*, 135-146.

(36) Giacobini, E. In *Handbook of Neurochemistry*; 2nd ed.; A. Lajtha, Ed.; Plenum: New York, 1983; Vol. 3; pp 583-605.

(37) Trijbels, J. M. F.; Monnens, L. A. H.; Bakkeren, J. A. J. M.; Van Raay-Selten, A. H. J.; Cortiaensen, J. M. B. *J. Inher. Metab. Dis.* **1979**, *2*, 39-42.

(38) Woody, N. C.; Pupene, M. B. *Pediatr. Res.* **1970**, *4*, 89-95.

(39) Gatfield, P. D.; Taller, E.; Hinton, G. G.; Wallace, A. C.; Abdelnour, G. M.; Haust, M. D. *Can. Med. Assoc. J.* **1968**, *99*, 1215-1233.

(40) Kinzel, J. J.; Bhattacharjee, J. K. *J. Bacteriol.* **1979**, *138*, 410-417.

(41) Kinzel, J. J.; Bhattacharjee, J. K. *J. Bacteriol.* **1982**, *151*, 1073-1077.

(42) Fangmeier, N.; Leistner, E. *J. Biol. Chem.* **1980**, *255*, 10205-10209.

(43) Gilbertson, T. J. *Phytochemistry* **1972**, *11*, 1737-1739.

(44) Fangmeier, N.; Leistner, E. *J. Chem. Soc., Perkin I* **1981**, 1769-1772.

(45) Mihalik, S. J.; Rhead, W. J. *J. Biol. Chem.* **1989**, *264*, 2509-2517.

(46) Mihalik, S. J.; Rhead, W. J. *J. Comp. Physiol. B* **1991**, *160*, 671-675.

(47) Mihalik, S. J.; McGuinness, M.; Watkins, P. A. *J. Biol. Chem.* **1991**, *266*, 4822-4830.

(48) Wanders, R. J. A.; Romeyn, G. J.; Schutgens, R. B. H.; Tager, J. M. *Biochem. Biophys. Res. Commun.* **1989**, *164*, 550-555.

(49) Broquist, H. P. *Annu. Rev. Nutr.* **1991**, *11*, 435-448.

(50) Rao, V. V.; Tsai, M. J.; Pan, X.; Chang, Y. F. *Biochim. Biophys. Acta* **1993**, *1164*, 29-35.

(51) Huh, J. W.; Yokoigawa, K.; Esaki, N.; Soda, K. *Biosci. Biotech. Biochem.* **1992**, *56*, 2081-2082.

(52) Bradford, M. *Anal. Biochem.* **1976**, *72*, 248-254.

(53) Laemmli, U. K. *Nature* **1970**, *227*, 680-685.

(54) Loewenstein, J.; Scholte, H. R.; Wit-Peeters, E. M. *Biochim. Biophys. Acta* **1970**, *223*, 432-436.

(55) Ornstein, L. *Annal. NY Acad. Sci.* **1964**, *121*, 321-349.

(56) Davis, B. J. *Annal. NY Acad. Sci.* **1964**, *121*, 404-427.

(57) Jovin, T. *Biochemistry* **1973**, *12*, 879-890.

(58) McLellan, T. *Anal. Biochem.* **1982**, *126*, 94-99.

(59) Moos, M.; Nguyen, N. Y.; Liu, T. Y. *J. Biol. Chem.* **1988**, *263*, 6005-6008.

(60) Witwer, A. J.; Wagner, C. *J. Biol. Chem.* **1981**, *256*, 4109-4115.

(61) Rodwell, V. W. In *Methods in Enzymology*; H. Tabor and C. H. Tabor, Ed.; Academic Press: New York, 1971; Vol. 17B; pp 174-188.

(62) Kelley, W.; Zabriskie, T. M. unpublished results.

(63) Pecci, L.; Costa, M. *J. Chromatogr.* **1988**, *426*, 183-187.

(64) Einarsson, S. *J. Chromatogr.* **1985**, *348*, 213-220.

(65) Silverman, R. B.; Zieske, P. A. *Biochemistry* **1985**, *24*, 2128-2138.

(66) Rao, V. V.; Chang, Y. F. *Biochim Biophys Acta* **1992**, *1139*, 189-195.

(67) BioRad *Model 491 Prep Cell Instruction Manual*; 1994.

(68) Witwer, A. J.; Wagner, C. *J. Biol. Chem.* **1981**, *256*, 4102-4108.

(69) Brown, E. D.; Wood, J. M. *J. Biol. Chem.* **1992**, *267*, 13086-13092.

(70) Menzel, R.; Roth, J. *J. Biol. Chem.* **1980**, *256*, 9755-9766.

(71) Johnson, A. B.; Strecker, H. J. *J. Biol. Chem.* **1962**, *237*, 1876-1882.

(72) Kelley, W.; Liang, X.; Zabriskie, T. M. unpublished results.

(73) Mihalik, S. J.; McGuiness, M. C. In *Flavins and Flavoproteins* Walter de Gruyter & Co.: Berlin, 1990; pp 881-884.

(74) Silverman, R. B. *Acc. Chem. Res.* **1995**, *28*, 335-342.

(75) Edmondson, D. E.; Bhattachargya, A. K.; Walker, M. C. *Biochemistry* **1993**, *32*, 5196-5202.

(76) Liang, X.; Zabriskie, T. M. unpublished results.

(77) Qi, H.; Zabriskie, T. M. unpublished results.

(78) Zeller, H. D.; Hille, R.; Jorns, M. S. *Biochemistry* **1989**, *28*, 5145-5154.

(79) Bernardi, F.; Epiotis, N. D.; Cherry, W.; Schiegel, H. B.; Whangbo, M. H.; Wolfe, S. *J. Am. Chem. Soc.* **1976**, *98*, 469-478.

(80) Ioto, O.; Matsuda, M. In *Chemical Kinetics of Small Organic Radicals*; Z. B. Alfassie, Ed.; CRC Press, Inc.: Boca Raton, 1988; Vol. 3; pp 133-164.

(81) Zabriskie, T. M. *J. Med. Chem.* **1996**, *3938*, 0000.

(82) Kim, M. S.; Zabriskie, T. M. unpublished results.